Superheavy Nuclei in the Relativistic Mean Field Theory

G.A. Lalazissis[1,4], M.M. Sharma[2], P. Ring[1] and Y.K. Gambhir[3]

[1]Physik Department, Technische Universität München
D-85747 Garching, Germany
[2]Max Planck Institut für Astrophysik,
D-85740 Garching bei München, Germany
[3]Physics Department, I.I.T. Powai, Bombay 400076, India
[4]Department of Theoretical Physics, Aristotle University of Thessaloniki,
GR 54006 Thessaloniki, Greece.

February 9, 2008

Abstract

We have carried out a study of superheavy nuclei in the framework of the Relativistic Mean-Field theory. Relativistic Hartree-Bogoliubov (RHB) calculations have been performed for nuclei with large proton and neutron numbers. A finite-range pairing force of Gogny type has been used in the RHB calculations. The ground-state properties of very heavy nuclei with atomic numbers Z=100-114 and neutron numbers N=154-190 have been obtained. The results show that in addition to N=184 the neutron numbers N=160 and N=166 exhibit an extra stability as compared to their neighbors. For the case of protons the atomic number Z=106 is shown to demonstrate a closed-shell behavior in the region of well deformed nuclei about N=160. The proton number Z=114 also indicates a shell closure. Indications for a doubly magic character at Z=106 and N=160 are observed. Implications of shell closures on a possible synthesis of superheavy nuclei are discussed.

1 Introduction

Exploration of the domain of superheavy nuclei has been pursued for a long time and limits on stability and feasibility of creating superheavy nuclei have been tested time and again. This pursuit has been enlivened by the constant hope of creating nuclei having mass and charge much larger than those we are familiar with. The shell effects which play a major role in creating nuclei with magic numbers and thus provide a higher stability have increased the hope of being able to create superheavy nuclei. Theoretically, various schemes have been adopted to calculate shell effects in the unknown teritorry of superheavies [1, 2, 3] and at the same time superheavy nuclei have evoked an enormous experimental interest. Recent discoveries of several new elements and the ability of the experimentalists to synthesize heavy nuclei with atomic numbers Z=109-112 have added to the momentum of the activity in the pursuit of the superheavy nuclei [4, 5, 6, 7, 8, 9, 10]. However, an increase in the charge of a nucleus by every unit renders the nuclei increasingly unstable and consequently the ensuing nuclei live for a far shorter time than those with a correspondingly lower charge. Notwithstanding enormous difficulties in the synthesis and detection of these highly rare entities, experimental efforts are being made currently at the laboratories in GSI, GANIL, Berkeley and Dubna.

Recently, the production and decay of the heavy element $^{269}112$ have been reported [10] by the GSI group. Using a different experimental setup the Dubna-Livermore collaboration has discovered [11, 12, 13] new isotopes $^{265}106$, $^{266}106$ and $^{273}110$ and has measured their decay properties. It has been inferred that there is an enhanced nuclear stability in the vicinity of the deformed shells N=162 and Z=108. Nuclei in this region have been predicted to be extra stable by some theories. Accordingly experimental efforts are currently being devoted to explore the region about Z=108-116.

Theoretically, it is expected that a magic proton number should exist at Z=114. These predictions are based primarily upon phenomenological models such as finite-range droplet model (FRDM) [3]. In addition to predicting major shell gaps at Z=114 and N=184, the FRDM also predicts larger shell gaps at proton numbers Z=104, 106, 108 and 110 at neutron numbers N=162 and 164. A prolate deformation in this region has been surmised

for these nuclei [3]. For a search of superheavy nuclei, theories based upon Nilsson-Strutinsky scheme [14, 15, 2] have also been employed extensively. A similar pattern of deformed nuclei have been predicted about Z=108 and N=162 in this approach as in FRDM. In addition, microscopic calculations [16, 17, 18, 19] have also been attempted in this region. However, the main obstacle which the theories including those of the macroscopic nature face is the question whether the approaches which apply to the region of beta-stability line can be extrapolated to such very heavy systems.

Shell effects play a key role for the very existence of magic nuclei. Such shell effects manifest strongly along the line of stability in the form of much higher stability of magic nuclei and thus a higher abundance of such elements as compared to their neighbors. A semblance of the same would be affected also for superheavy nuclei, if there were any magic numbers in this region. Consequently, these nuclei will be guarded against a faster decay by fission as compared to their non-magic counterparts. Synthesis of superheavy nuclei is thus subject to the interplay of the shell effects in the region of very heavy nuclei.

The Relativistic Mean-Field (RMF) theory has recently proven to be a very powerful tool for an effective microscopic description of the ground-state properties of nuclei [18, 20, 21, 22, 23, 24]. The RMF theory has also been successful in describing the properties of nuclei which entail shell effects. Examples where shell effects play an important role and where the RMF theory has shown a remarkable success are the description of the anomalous isotope shifts of many nuclei from Z=40 region [22] to the rare-earth nuclei [23] and the most notable case of Pb nuclei [25]. A description of the deformation properties and the complex series of shape transitions in many isotopic chains has also been achieved [23], where results including those with very large isospins match the predictions of the exhaustive mass models FRDM and ETF-SI (Extended Thomas-Fermi and Strutinsky Integral). Thus, the RMF theory has achieved a great success in providing a unified description of the binding energies and deformation properties of nuclei all over the periodic table including exotic nuclei. This gives an added confidence in the RMF theory to employ and extrapolate it in the region of the superheavy nuclei. It is noteworthy that the RMF theory with scalar self-coupling employs only 6 parameters. This is in contrast

with the macroscopic-microscopic approaches which use a considerably large number of parameters fitted extensively to a large body of nuclear data.

Usually pairing correlations are taken into account only in a very phenomenological way using occupation numbers of the BCS type based on empirical pairing gaps deduced from odd-even mass differences. This procedure works well in the valley of beta-stability, where experimental masses are known. The predictive power for pairing gaps for nuclei far from the line of beta stability and for superheavy nuclei is thus limited. We have, therefore, extended relativistic mean-field theory to relativistic Hartree-Bogoliubov theory [26] whereby we use a pairing force of finite range, similar to that of the well established Gogny type in non-relativistic calculations.

Using this pairing interaction we investigate the possible existence of proton (neutron) shell closures in the region of the super heavy nuclei, where it is well known that the role of pairing is important. In our calculations we have adopted the RMF force NL-SH [21] which is especially suitable for exotic nuclei as it takes into account the isospin dependence correctly.

In the present paper, we investigate the ground-state properties of nuclei in the region of a plausible existence of superheavy nuclei. We have undertaken extensive calculations for nuclei over a large range of atomic charge and mass. In section 2 we describe some essential features of the RMF theory. We give numerical and other details in section 3. In section 4 results of the RMF calculations are provided and discussed. A comparison of our results is made with the predictions of other models wherever possible. In the last section we discuss our results vis-a-vis experimental data available to-date and summarize our main conclusions.

2 The Relativistic Mean-Field Theory

The basic Ansatz of the RMF theory is a Lagrangian density [27, 28] whereby nucleons are described as Dirac particles which interact via the exchange of various mesons. The

Lagrangian density can be written in the form:

$$\begin{aligned}\mathcal{L} &= \bar{\psi}(i\partial\!\!\!/ - M)\psi + \tfrac{1}{2}\partial_\mu\sigma\partial^\mu\sigma - U(\sigma) - \tfrac{1}{4}\Omega_{\mu\nu}\Omega^{\mu\nu} + \\ &\tfrac{1}{2}m_\omega^2\omega_\mu\omega^\mu - \tfrac{1}{4}\vec{R}_{\mu\nu}\vec{R}^{\mu\nu} + \tfrac{1}{2}m_\rho^2\vec{\rho}_\mu\vec{\rho}^\mu - \tfrac{1}{4}F_{\mu\nu}F^{\mu\nu} \\ &g_\sigma\bar{\psi}\sigma\psi \;-\; g_\omega\bar{\psi}\omega\!\!\!/\psi \;-\; g_\rho\bar{\psi}\vec{\rho}\!\!\!/\vec{\tau}\psi - \; e\bar{\psi}A\!\!\!/\psi\end{aligned} \tag{1}$$

The meson fields included are the isoscalar σ meson, the isoscalar-vector ω meson and the isovector-vector ρ meson. The latter provides the necessary isospin asymmetry. A correct isovector coupling constant is important for describing the properties of nuclei over a large range of isospins. The arrows in Eq. (1) denote the isovector quantities. The Lagrangian contains also a non-linear scalar self-interaction of the σ meson :

$$U(\sigma) \;= \frac{1}{2}m_\sigma^2\sigma^2 \;+\; \frac{1}{3}g_2\sigma^3 \;+\; \frac{1}{4}g_3\sigma^4 \tag{2}$$

The scalar potential (2) is essential for appropriate description of surface properties [29]. M, m_σ, m_ω and m_ρ are the nucleon-, the σ-, the ω- and the ρ-meson masses respectively, while g_σ, g_ω, g_ρ and $e^2/4\pi = 1/137$ are the corresponding coupling constants for the mesons and the photon.

The field tensors of the vector mesons and of the electromagnetic field take the following form:

$$\Omega^{\mu\nu} = \;\; \partial^\mu\omega^\nu - \partial^\nu\omega^\mu \tag{3}$$

$$\tag{4}$$

$$\vec{R}^{\mu\nu} = \;\; \partial^\mu\vec{\rho}^\nu - \partial^\nu\vec{\rho}^\mu \tag{5}$$

$$\tag{6}$$

$$F^{\mu\nu} = \;\; \partial^\mu A^\nu - \partial^\nu A^\mu \tag{7}$$

The variational principle gives the equations of motion. In our approach, where the time reversal and charge conservation is considered, the Dirac equation for the static case is written as:

$$\{-i\alpha\nabla + V(\mathbf{r}) + \beta[M + S(\mathbf{r})]\}\psi_i \;=\; \varepsilon_i\psi_i, \tag{8}$$

where $V(\mathbf{r})$ represents the vector potential:

$$V(\mathbf{r}) = g_\omega\omega_0(\mathbf{r}) + g_\rho\tau_3\rho_0(\mathbf{r}) + e\frac{1+\tau_3}{2}A_0(\mathbf{r}), \tag{9}$$

and $S(\mathbf{r})$ is the *scalar* potential:

$$S(\mathbf{r}) = g_\sigma \sigma(\mathbf{r}) \tag{10}$$

the latter contributes to the effective mass as:

$$M^*(\mathbf{r}) = M + S(\mathbf{r}). \tag{11}$$

The Klein-Gordon equations for the meson fields are time-independent inhomogeneous equations with the nucleon densities as sources.

$$\begin{aligned}
\{-\Delta + m_\sigma^2\}\sigma(\mathbf{r}) &= -g_\sigma \rho_s(\mathbf{r}) - g_2\sigma^2(\mathbf{r}) - g_3\sigma^3(\mathbf{r}) && (12)\\
\{-\Delta + m_\omega^2\}\omega_0(\mathbf{r}) &= g_\omega \rho_v(\mathbf{r}) && (13)\\
\{-\Delta + m_\rho^2\}\rho_0(\mathbf{r}) &= g_\rho \rho_3(\mathbf{r}) && (14)\\
-\Delta A_0(\mathbf{r}) &= e\rho_c(\mathbf{r}) && (15)
\end{aligned}$$

The corresponding source densities are obtained as

$$\begin{aligned}
\rho_s &= \sum_{i=1}^{A} \bar{\psi}_i \; \psi_i \\
\rho_v &= \sum_{i=1}^{A} \psi_i^+ \; \psi_i \\
\rho_3 &= \sum_{p=1}^{Z} \psi_p^+ \; \psi_p \; - \; \sum_{n=1}^{N} \psi_n^+ \; \psi_n \\
\rho_c &= \sum_{p=1}^{Z} \psi_p^+ \; \psi_p
\end{aligned} \tag{16}$$

where the sums are taken over the valence nucleons only. In the present approach contributions from negative-energy states are neglected (*no-sea* approximation), i.e. the vacuum is not polarized. Thus, we work within the framework of the non-linear $\sigma\omega$ model which includes the scalar self-coupling up to quartic order.

3 Details of the Calculations

Calculations for superheavy nuclei have been performed using the oscillator expansion method. The details of the method have been provided in our earlier papers (for example

see Ref. [18]). Most of our earlier calculations were carried out using 20 oscillator shells for spherical nuclei and 12 or 14 oscillator shells for deformed nuclei. In the present case of very heavy nuclei we have used 20 shell for spherical as well as for deformed nuclei.

It is well known that pairing correlations play an important role in our understanding of structure of nuclei with open shells. Using Green's function techniques and Gorkov's factorization one can derive in principle a relativistic theory of pairing correlations [26]: Starting from a Lagrangian containing nucleonic spinors and meson fields one obtains relativistic Hartree-Bogoliubov equations. If one uses the same parameters for the mesons in the particle-particle channel as in the relativistic mean-field theory, a quantitative description of pairing is, however, not possible. The large values of the σ- and ω-mass lead to relatively short-range interactions which produce much too strong pairing correlations. Thus, in the relativistic theories one is faced with the same problem as with Skyrme forces, i.e. one needs cut off parameters in the particle-particle channel. In principle, however, there is no reason why one should use the same effective interaction in both the channels. At present there is no microscopic derivation of the effective interaction responsible for particle-particle correlations. However, in many cases the simple monopole pairing force with constant pairing matrix elements in a certain region around the Fermi surface turns out to yield very satisfactory results, if the pairing force constant G is adjusted to the experimental gap parameter deduced from the odd-even mass differences. This prescription is used in many ways, for instance, in Nilsson-Strutinsky calculations, in density-dependent Hartree-Fock calculations with Skyrme forces and also in the relativistic mean-field theory. Thus, in this procedure one ends up with rather different pairing force constants G in the different regions of the periodic table. In fact, the size of this constant depends on the pairing cut off. On the other hand, Gogny's parameterization of an effective force based on two Gaussians with a finite range provides a unified phenomenological description without a cut-off parameter of pairing properties across a large part of the periodic table[30]. This method is considered to work satisfactorily in the region of medium and heavy nuclei.

In this paper, we therefore use in the particle-particle channel a finite-range force of

the Gogny type This force consists of a sum of two Gaussians,

$$V^{pp}(1,2) \;=\; \sum_{i=1,2} e^{-\left(\frac{\boldsymbol{r}_1-\boldsymbol{r}_2}{\mu_i}\right)^2} \left(W_i \;+\; B_i P^{\sigma} - H_i P^{\tau} - M_i P^{\sigma} P^{\tau}\right), \qquad (17)$$

with the parameters μ_i, W_i, B_i, H_i, and M_i $(i = 1, 2)$. a short-range repulsive term and a medium-range attractive term. We neglect the density-dependent part and the spin-orbit part of the Gogny force, because the density-dependent part vanishes in the $S = 0$, $T = 1$ channel and the latter gives only relatively small contributions. Since we are working in an oscillator basis, we can use the very elegant and simple techniques introduced by Talman [31] in order to evaluate the Gaussian matrix elements in a spherical basis. In this paper, we use the parameter set D1 for the pairing force as given in Ref. [30] and are listed in Table 1.

Calculations have also been performed for a set of nuclei in a cylindrically symmetric deformed configuration. So far we have not implemented the evaluation of the Gogny matrix elements in the axially deformed bases. We therefore use for the deformed calculations the usual BCS formalism with constant pairing gaps obtained from the prescription of Ref. [32]. In these calculations also we have now included 20 oscillator shells both for the fermionic as well as bosonic wave functions. The calculations have been carried out only for a selected set of nuclei in view of an enormously large computation time required for a Hartree minimization in a deformed basis with 20 shells.

In our study the force NL-SH [21] has been used. The parameters of NL-SH are given in Table 2. It has been shown that NL-SH reproduces a wide variety of nuclear data all over the periodic table. The shell effects and an appropriate symmetry energy contained in this force are responsible for describing various data successfully.

4 Results and Discussion

4.1 Particle Separation Energies

The present study of superheavy nuclei spans even-even nuclei with atomic numbers $100 \leq Z \leq 118$ and neutron numbers $154 \leq N \leq 190$. First, we present the results of the relativistic Hartree-Bogoliubov (RHB) calculations for nuclei with $158 \leq N \leq 190$

assuming a spherical configuration and employing the force NL-SH. In these calculations the finite-range pairing force of the Gogny type has been used for pairing as discussed above. This minimizes the uncertainties in the pairing

For the sake of a clear presentation of the results the neutron range 158-190 has been divided into two parts, 158-176 and 178-190. Fig. 1 (a) shows the two-neutron separation energies S_{2n} for nuclei with N=158-176 for the whole range of the atomic number Z=100-114. Each curve corresponds to an isotopic chain for a given Z. The lowest curve is for Z=100 and the highest one corresponds to Z=114. Clearly, with an increase in the neutron number, the S_{2n} values show a regular decrease except at N=164-166, where a slight discontinuity in the two-neutron separation energies can be seen. This discontinuity is more pronounced above Z=110. Such discontinuities are symptomatic of shell effects which prevail all over the periodic table. Similar effects emerge also in the compilation of recent empirical masses in Ref. [33], where clear discontinuities at the known magic numbers can be seen. In the present case, nuclei above N=164 become increasingly vulnerable to neutron decay due to a fast decrease in the S_{2n} values. This is indicative of an enhanced stability for nuclei with N=164. The curve for Z=106, in contrast, shows an increase in S_{2n} value at N=166. This indicates that the nucleus with N=166 and Z=106 is slightly more stable against neutron decay.

The two-neutron separation energies in the RMF theory for the second range of neutrons N=178-190 are shown in Fig. 1 (b). The curves for the range of the proton numbers Z=100-114 are shown. The lowest curve corresponds to Z=100 and the highest one is for Z=114. A strong kink in the S_{2n} values is clearly visible for the curves Z=100-108 at N=184. The kink for the other Z values decreases slightly and it becomes relatively much smaller at Z=114. This kink at N=184 for all Z values underlines the manifestation of a magic number at N=184. The shell-closure at N=184 is consistent with the predictions of other theoretical models such as Nilsson-Strutinsky and finite-range droplet model (FRDM) [34], whereby a strong shell-closure at this neutron number has been suggested.

The two-proton separation energies S_{2p} obtained in the RMF theory for nuclei with Z=102-114 are shown in Fig. 2 (a). Each curve corresponds to a given neutron number

which changes from N=156 to N=178 in going from the bottom to the top of the figure. A decreasing trend with an increase in the atomic number is to be seen clearly. The S_{2p} values also show an obvious decrease in the values with a decrease in the neutron number. However, a small kink in the S_{2p} values at Z=106 for the neutron numbers N=156-160 is observed. This kink is reduced as one proceeds to neutron numbers higher than N=156 and it vanishes for nuclei above N=160. Thus, spherical calculations for these nuclei demonstrate the existence of a large shell gap at Z=106 with neutron numbers N=156-160. This shell gap in the proton number is washed out in going to higher neutron numbers. In section 4.6 on shell corrections, it will be shown that the shell correction energies do corroborate to a magic like character for Z=106 for neutron numbers about N=160.

The corresponding S_{2p} values for nuclei with higher neutron numbers N=180-188 are shown in Fig. 2 (b). The values show a monotonous decrease with an increase in proton number. There is no kink to be seen in the S_{2p} values. Thus, for nuclei with even higher neutron numbers than those shown in Fig. 2 (a), the spherical calculations do not show any magic proton number except for Z=114, where a slight change in the slope is indicated.

For the sake of a qualitative comparison, results obtained on the two-neutron separation energies in the FRDM are shown in Figs. 3 (a)-(b). A kink about N=162 and N=184 is seen clearly in both the figures. A similar feature was also predicted in density-dependent Skyrme theory [16]. On the conclusion that N=184 is a magic number, various theories including the RMF theory as well as other non-relativistic approaches are unanimous. In comparison, the mass model Extended Thomas-Fermi with Strutinsky Integral (ETF-SI) [35], which is based upon the Skyrme Ansatz, does not exhibit any clear signature for the magicity about N=162. However, it does show a slight kink in the S_{2n} values at about N=184, as can be seen in Figs. 4 (a) and (b).

The scenario for the mass models FRDM and ETF-SI is different as far as S_{2p} values are concerned. In the FRDM, the S_{2p} values show hardly any kink about Z=106 (Fig. 3(c)). Probably it is because the FRDM predicts larger shell gaps for the proton numbers

at Z=104, 106, 108 and 110 consecutively and as a result indications of a discontinuity amid these proton numbers seem to disappear. This is, however, different with the RMF predictions, where evidence for a 'magic' proton number at Z=106 was obtained for neutron numbers in the region of N=160. The FRDM values, on the other hand, show a clear kink only at Z=114 for higher neutron numbers about N=184 (Fig. 3(d)). The ETF-SI values, in contrast with FRDM, show a clear kink at Z=106 for lower neutron numbers N=156-166 (Fig. 4(c)). There is, however, no kink around Z=114 for higher neutron number such as N=184 (Fig. 4(d)). This observation in the ETF-SI is at odds with most of the theories which predict a strong magic number at Z=114. However, it should be noted that the recent density dependent Hartree-Fock-Bogoliubov calculations with the Skyrme force SkP [19] also does not predict a magic number at Z=114.

4.2 Pairing Energy

Pairing energy provides a reliable indication of magicity of a particle number. For magic nuclei, single-particle levels up to Fermi energy are fully occupied and hence there is no smearing of the Fermi surface. This implies that in such cases pairing is non-existent and hence the pairing energy should vanish. This feature is usually reflected in the sequence of the single-particle levels followed by a large gap in the levels near the Fermi energy.

In our self-consistent relativistic Hartree-Bogoliubov calculations, we have used finite-range pairing of the Gogny type, whereby the particle levels and the pairing fields are calculated self-consistently. The corresponding pairing energies for neutrons and protons as obtained in the RHB calculations are shown in Figs. 5 and 6, respectively.

The neutron pairing energies for several chains of nuclides with Z=100 to Z=114 are given in Fig. 5. A very strong peak in the pairing energy is observed at N=184 for all the atomic numbers. The pairing energy for all the nuclei with N=184 is seen to be zero. This fact is in accord with a strong kink observed in the S_{2n} values at N=184 as shown in Fig. 1 (b). Thus, it is demonstrated that the neutron number N=184 constitutes a very strong magic number. In addition, we also observe two other peaks in the neutron pairing energy, albeit not so strong, at N=164 and N=172. These peaks are highest

for Z=114. The peak structure at the above neutron numbers diminishes gradually in going down from Z=114 to Z=100. Comparatively, the peak at N=164 still remains up until Z=100, whereas the peak at N=172 disappears fast in going down to lower atomic numbers. As regards to the magnitude of the pairing energy for N=164 and N=172, it is seen that the pairing energy does not vanish even for Z=114 whereby the peak structure is most prominent amongst various atomic numbers. The lowest pairing energy at N=164 is about -1.0 MeV for the Z=114 nuclide. This value of the pairing energy is very small and indicates that the neutron pairing in this case is minimal. Thus, the results of Fig. 5 provide a good indication for the neutron number N=164 showing a relatively strong magicity.

The corresponding proton pairing energy is shown for nuclear chains from N=156 to N=190 in Fig. 6. A very strong peak at Z=106 is observed. The proton pairing energy vanishes at Z=106 for most of the nuclides with N=156 to N=164. The pairing energy for nuclei with Z=104 or Z=108 is 4-6 MeV larger and the pairing energy increases even further in going away from Z=106. This emphasizes the predominance of the Z=106 peak in the proton pairing energy. Thus, Z=106 turns out to possess a strong magic character. It is noteworthy that for nuclei with neutron numbers higher than N=164, the pairing energy is no longer zero and the peak at Z=106 vanishes. Thus, Z=106 does not show a magic character for higher neutron numbers. In conjunction with the neutron pairing energies of Fig. 5, we find that the nucleus with Z=106 and N=164 behaves like a doubly magic nucleus. An additional small peak is observed at Z=114 indicating a small magicity at this proton number.

4.3 Alpha-decay Half-Lives

Alpha decay is one of the most predominant modes of decay of superheavy nuclei. Depending upon the region of an extra stability which would originate from shell gaps and magicity, the half-life of the alpha decay is another indicator about a possible valley of stability. For an area of enhanced stability, the alpha-decay half-lives are expected to be longer than its neighbors. With this view, we calculate the alpha-decay half-lives for

several isotopic chains. We employ the phenomenological formula of Viola and Seaborg [36] for calculation of α half-lives:

$$\log T_\alpha = (aZ + b)Q_\alpha^{-1/2} + (cZ + d) \tag{18}$$

where Z is the atomic number of the parent nucleus and Q_α is the alpha-decay energy in MeV. T_α is then given in seconds. The parameters a, b, c, and d are taken from Ref [37], where these have been readjusted in order to take into account new data. The explicit values for these parameters are: a=1.66175, b=-8.5166, c=-0.20228, and d=-33.9069.

In Fig. 7 we plot the half lives T_α using the Viola and Seaborg [36] systematics. The logarithm of the half lives is shown for each isotopic chain in the region Z=102-118. One observes an enhancement in the $\log T_\alpha$ values at N=164 followed by a decrease at N=166 for most of the chains. The peak at N=164 emerges clearly in going to higher atomic numbers above Z=108. Thus, the neutron number N=164 would support synthesis of superheavy nuclei above Z=108.

Another maximum in the half-lives is seen at N=184. This is accompanied by a strong plateau up until N=184 for nuclei with lower atomic numbers. This plateau is followed by a strong dip at N=186 for nuclei below Z=112. The sudden and drastic change in the alpha-decay half-lives at N=186 is a strong indication of the magicity of N=184. Thus, the T_α values indicate regions of extra stability in the vicinity of N=164 and N=184, whereby the magicity of N=184 has been demonstrated unambiguously.

It should be noted that the half-lives T_α shown in Fig. 7 are obtained from the spherical RHB calculations. However, as we will see in the next section, some of these nuclei are deformed and therefore some of the Q_α-values may change slightly. Even a slight change in the Q_α's may produce half-lives T_α different by orders of magnitude. Therefore Fig. 7 should be regarded only as an indicative of the general trend.

4.4 Calculations with Deformed Configurations

In most of our previous investigations, calculations for deformed nuclei have been limited to a maximum of 14 deformed oscillator shells in the expansion, constrained mainly by

computational reasons. For nuclei not so heavy in charge and mass, calculations with 12 or 14 shells do produce reliable results. An extension of the deformed RMF calculations by taking into account higher number of oscillator shells up to 20 is extremely time consuming. Therefore, deformed calculations for the whole of the superheavy regions with 20 oscillator shells put a heavy burden on computation. In view of this, we have selected a region of superheavy nuclei about the neutron number N=164 and another one about N=184 for axially deformed RMF calculations with 20 shells. Pairing correlations are included in the constant gap approximation. The pairing gaps used in the calculations were obtained from the prescription of Ref. [32].

The region with N=164 is likely to yield nuclei with a reasonable deformation, whereas the latter region with N=184 being a strong magic number is likely to provide nuclei with an almost spherical shape. Results of the axially deformed RMF calculations are shown in Table 3, where the quadrupole and hexadecupole deformations β_2 and β_4, respectively, are shown for several isotopic chains. The β_2 and β_4 values are obtained from the quadrupole and hexadecupole moments using the method of Ref. [38].

The nuclei given in Table 3 have been selected with a view to be able to calculate alpha-decay half-life of nuclei around N=164. The calculations encompass a few isotopes of nuclei with Z=102 and Z=110-112, whereas calculations for many more isotopes have been performed for nuclei with other atomic numbers. Predictions on the quadrupole and hexadecupole deformations in the FRDM and ETF-SI mass models are also shown for comparison. It is observed that most of the nuclei in this region are well deformed. The β_2 values obtained in the RMF theory are close to those of FRDM for most of the cases and both the RMF theory and FRDM show a similar trend as a function of mass number. On the other hand, the ETF-SI model seems to be using a rather fixed value of β_2 for most of the nuclei in a given chain. Therefore, a comparison of the RMF values with the ETF-SI values is not meaningful. On the whole, the RMF theory as well as the mass models, all predict a prolate shape for all the nuclei in this region.

The β_4 values obtained in the RMF theory for all the nuclei in Table 3 are negative. These values in the RMF theory are comparable to those in the FRDM. Moreover, the

RMF theory predicts the same sign (negative) for the hexadecupole deformation as does the FRDM. The β_4 values in the ETF-SI are also negative for most of nuclei with only a few exceptions for heavy nuclei with $A > 276$. Thus, the RMF hexadecupole moments are by and large in good conformity with the existing mass models.

The two-neutron separation energies (S_{2n}) and alpha-decay half-lives (T_α) obtained from the deformed RMF calculations are shown in Fig. 8 for the isotopic chains of Z=106 and Z=108. The S_{2n} values show a usual decrease with an increase in neutron number. The Z=108 curve does not show any structure about N=164, whereas Z=106 values do show a kink about N=166. Thus, S_{2n} values for Z=106 show an indication of some magicity about N=164-166. The alpha-decay half-lives also display a clear structure above N=164 and exhibit a significant enhancement in the T_α value for nuclides with N=166 both for Z=106 as well as for Z=108. Thus, an extra stability is shown by both the nuclei ^{272}106 and ^{274}108. Nuclei with N=168 show a slight decrease in the T_α value as compared to nuclei with N=166. However, the T_α value for N=168 is considerably higher than for nuclei with neutron numbers below N=166. Thus, these values signify an area of an added stability about N=166. It is to be remarked that the values of T_α shown in Fig. 8 differ from the corresponding values displayed in Fig. 7 due to slightly different values of Q_α obtained in the deformed calculations.

Several recent experiments have been able to measure energy of α-particles emitted in decay of superheavy nuclei. In order to facilitate a comparison of the theoretical predictions with experimentally observed alpha-decay energies, we show in Fig. 9, the Q-value for alpha decay, i.e., Q_α for the isotopic chains with Z=106 and Z=108. The RMF theory predicts that the isotopes with Z=106 would decay with an α-particle energy of about 7-8 MeV, whereas nuclei in the isotopic chain with Z=108 would decay with an α-particle energy of about 9-10 MeV. The measured energy of the emitted α particle is 8.63 MeV for ^{266}106 and the corresponding energy for the case of Z=108 is between 9.7 - 9.87 MeV. These numbers are in close conformity with the calculated Q_α shown in Fig. 9. A further comparison of these values with recent experimental observations will be made in the last section.

In order to check the sphericity of nuclei in the vicinity of N=184, we have performed RMF calculations in a deformed basis also for several nuclei with N=184 by taking into account 20 oscillator shells. The nuclei considered are isotones of N=184 with mass numbers A=290, 292, 294 and 298. The binding energies and quadrupole deformations obtained in the RMF calculations are shown in Table 4. The predictions of FRDM and ETF-SI both on binding energies as well as on deformations are also shown for comparison. The RMF theory predicts the quadrupole deformation of these nuclei to be very close to zero. Thus, the RMF theory and mass models both predict a spherical shape for nuclei with N=184. It may be emphasized that moving away from the region of a strong deformation about N=166 towards N=184, the RMF theory produces nuclei which tend to become spherical as the neutron number 184 is approached. This is again an indication that the region about N=184 is associated with a magic number.

The binding energies obtained in the RMF theory are in good agreement with those of ETF-SI within 1-2 MeV, whereas the FRDM values differ from the RMF and ETF-SI values by only a few MeV. Thus, the RMF theory predicts binding energies which are very close to those of FRDM and ETF-SI.

4.5 Single-Particle Spectra of Superheavy Nuclei

The single-particle levels obtained in the deformed RMF calculations for several key nuclei are shown in Figs. 10-13 both for neutrons and protons. The levels correspond to the ground-state deformations as obtained in each calculation and which have been shown in Table 3. First, we show the single-particle spectra for isotopic chains with neutron numbers N=162-166 for the proton number Z=106 and Z=108 in Figs. 10-12. The numbers in the braces shown in the large shell gaps denote shell closures. The associated Fermi energies are also shown by dashed lines.

The single-particle (s.p.) spectrum for ^{268}106 (N=162) shown in Fig. 10 exhibits only a small gap at N=162. For protons a considerably larger gap at Z=106 in this nucleus can be seen. In the same figure, the neutron s.p. spectrum for the nucleus ^{270}108 (N=162) does not display any significant gap near N=162. A clear gap is, on the other hand, visible

at the neutron number N=166. Similarly, a major shell gap at proton number Z=108 is seen. Thus, the single-particle spectra for the above two isotones show a major shell gap at N=166 in neutrons and an equally strong shell gap in protons for both Z=106 and Z=108.

In Fig. 11 we examine the single-particle spectrum for isotones with N=164. For nuclei with Z=106 as well as Z=108, a clear gap in the neutron single-particle spectrum emerges at N=166. This is consistent with what we observed also in Fig. 10. Similarly, a reasonably good gap is to be seen for proton number Z=106 in the nucleus ^{270}106 as well as for Z=108 in the nucleus ^{272}108. In the single-particle spectrum for isotones with N=166 (Fig. 12), a very clear shell gap at neutron number N=166 can be seen. This gap is observed consistently in the single-particle spectra of nuclei with N=162, 164 and 166. This lends credence to the prediction that a major shell gap at N=166 should exist. This would consequently provide a region of extra stability centered about N=166.

The proton single-particle spectra for N=166 isotones show a gap at proton number 106 both for the nuclei with atomic numbers Z=106 as well as Z=108. Thus, the nucleus with N=166 and Z=106 can be construed as a 'double magic' nucleus in the landscape of deformed nuclei prevalent in this region.

Single-particle spectra for isotones of N=184 with Z=106, 108, 110 and 114 are shown in Fig. 13 both for neutrons and protons. A very clear and profound shell gap at N=184 is exhibited by neutron single-particle spectra for all the isotones. This is in conjunction with the fact that nuclei around N=184 are predominantly spherical in the RMF theory. This establishes the magicity of the neutron number N=184 unequivocally. At the same time it is observed that the shell gap at N=184 decreases slightly as one proceeds from Z=106 to Z=114. This may imply that though N=184 retains its magicity in going to higher atomic numbers, the magicity does show a decline towards higher atomic numbers. This may have a consequence that nuclei if synthesized about N=184 would tend to favor a charge value Z=106 rather than Z=114. For the latter a decreased stability stemming from a reduced shell gap at N=184 will ensue.

The proton single-particle spectra for N=184 isotones show a shell gap at Z=106

as well as at Z=114. It can be seen that the gap at Z=106 is not so strong vis-a-vis that observed for the major neutron shell-closure N=184. The shell gap at Z=114 is, in comparison, as strong as that exhibited by N=184. The gaps at Z=106 and at Z=114 are strong indications of shell closures in the proton mean field. Thus, Z=106 as well as Z=114 show signatures of magicity in the proton number. The nucleus with Z=106 and N=184 and the one with Z=114 and N=184 provide a semblance of doubly magic nuclei.

4.6 Shell Corrections

Shell corrections provide an indicator about the deviation in the structure of nuclei away from the smooth liquid-drop type of behavior. The magnitude of the shell correction signifies the role of shell effects at play in a nucleus. We have evaluated shell correction for a set of nuclei employing the Strutinsky procedure. The single-particle spectra of nuclei as obtained in the RMF theory have been used as an input for a smoothing procedure. Pairing has been duly taken into account in these calculations according to the prescription of Ref. [39].

The microscopic shell corrections obtained from the Strutinsky procedure applied to the single-particle spectra of the RMF theory are given in Table 5 for several nuclei. In these calculations we have covered many nuclei with neutron numbers from N=154 to N=168 and with proton numbers from Z=104 to Z=116. The table shows a significant negative shell correction suggesting an important role of the shell effects in this region. We scan the table row-wise. The first two rows, i.e. the shell corrections for Z=104 and Z=106 show a large minimum at -6.79 and -8.05 MeV, respectively. Both the minima correspond to N=160. This implies that there should exist a large shell gap at N=160. In the two-dimensional landscape of the shell correction, the shell energy shows a decrease from -6.79 MeV for Z=104 to -8.05 MeV for Z=106. The magnitude of the shell energies for neutron numbers less than N=160 in the first two rows is less than those for N=160. The values, however, still indicate a significant shell correction below N=160. For nuclei above N=162, shell correction energies are much smaller than for N=160. Moreover, the minimum at Z=106 and N=160 is the absolute minimum in the given table. Thus, the

nucleus $^{266}106$ with a large shell correction is expected to exhibit a reasonably higher stability as compared to its neighbors. This scenario is consistent with the experimental observation of the isotope $^{266}106$ and with its decay properties [11], where an indication of an extra stability in the superheavy nuclei has been conjectured.

Considering the shell corrections for nuclei above Z=106, i.e. the rows below the first two, the minimum in the energy shifts a slightly. For Z=108, a minimum occurs at N=158, which is a reasonably strong one. The shell correction energies for the next neighbors on both the sides of N=158 are smaller only by 0.2 MeV. Thus, all the nuclei with N=156, 158 and 160 and Z=108 are likely to possess reasonable shell gaps in the single-particle spectra and therefore an ensuing stability.

For nuclei above Z=108, the minimum branches off to N=158 and N=166. As the proton number increases above 110, the minimum at N=158 diminishes gradually into a local minimum and at the same time a stronger minimum develops at N=166. Thus, the neutron number N=158 does not benefit from the approaching Z=114 which is predicted to be a major magic number. On the contrary, nuclei with N=166 and Z=112, 114 could show a semblance of 'double magic' character in the island of deformation. The nucleus with N=166 and Z=112 has been shown to possess a quadrupole deformation $\beta_2 = 0.18$ (Table 3). The proton number Z=114, on the other hand, is expected to form a doubly magic spherical nucleus with its neutron counterpart at N=184, the region which is at present not yet accessible experimentally.

5 Summary and Conclusions

We have studied the ground-state properties of nuclei in the superheavy region with a view to explore possible regions of enhanced stability. Calculations have been carried out in the framework of the relativistic non-linear $\sigma\omega$ model with scalar self-coupling. First, we performed Hartree-Bogoliubov calculations using a spherical configuration in an oscillator basis with 20 shells. These calculations employ the finite-range pairing force of the Gogny type. It has been shown that the behavior of the two-neutron separation energies and the pairing energy of neutrons indicate a possible shell closure at N=164

and N=184 in the neutron number. In the proton number, the corresponding quantities suggest a possible shell closure at Z=106 and Z=114.

Nuclei in the region of the neutron number N=166 are expected to be deformed. Therefore, we have also performed RMF calculations for nuclei on both the sides of N=166 using an axially deformed configuration. These calculations use 20 oscillator shells, and the pairing has been included in the BCS formalism using constant pairing gaps. The calculations encompass atomic numbers from Z=102 to Z=114. It has been shown that nuclei in the region of N=166 acquire a reasonably strong quadrupole deformation of the prolate type. Nearly all the nuclei in this region exhibit a negative hexadecupole deformation. The RMF results show a very good agreement with the predictions of the mass formula FRDM both on the magnitude as well as on the sign of the quadrupole and hexadecupole deformations. The quadrupole and hexadecupole deformations in the RMF theory can also be compared reasonably well with the predictions of ETF-SI, where a constant value of β_2 and β_4 seems to have been used in this region of nuclei.

The half-lives of alpha-decay have been calculated from the results of the deformed RMF calculations. The results indicate a significant enhancement in the alpha-decay half-life about N=166 and thus the RMF theory predicts a region of an extra stability near N=166. This is consistent with the results obtained in the spherical calculations for the particle-separation energies. A possible enhancement in the alpha-decay half-lives is also observed at about Z=106-108 in the proton number. It is, however, difficult to say with certainty on the basis of alpha-decay half-lives only, whether Z=106 or Z=108 constitutes a possible shell closure.

The single-particle spectra help to provide a clue as to whether a particular particle number has a magic character or not. We have therefore examined the single-particle spectra obtained from deformed RMF calculations. The structure of the single-particle spectra reveals major shell gaps in neutrons at N=166 and at N=184. It may be recalled that in the spherical calculations a closed neutron shell was obtained at N=164. Thus, the deformation of nuclei in this region drives the closed shell from N=164 to N=166. On the other hand, the shell gap at the neutron number N=184 is shown unambiguously

also in the deformed calculations which lead to spherical nuclei. It is consistent with the predictions of the calculations in the spherical basis. It may be appropriate to say that the shell gap at N=166 would bear a strong significance to creating superheavy nuclei, as it indicates a 'semi-magic' nature for this neutron number.

The structure of the proton single-particle spectra, on the other hand, provides a signature for a seemingly major shell gap at Z=106. A shell gap at Z=108 is, however, not observed in the single-particle spectra. Thus, in the domain of protons, Z=106 is the only 'semi-magic' number predicted by the RMF theory in the region of lighter superheavy nuclei. This is slightly different from the results of the Nilsson-Strutinsky approach [2] which predicts a strong shell-closure in protons at Z=108.

It is noteworthy that the recent discovery of superheavy nuclei ^{265}106, ^{266}106 [11] and ^{267}108 [12] and measurements of the associated properties shed a considerable light on some of the issues related to this unknown region. The Dubna-Livermore collaboration has observed [11] the alpha-decay half-life of the above Z=106 isotopes to be 2-30 s and 10-30 s, respectively. The corresponding alpha-decay energies have also been measured and have been found to be 8.71-8.91 MeV and 8.63 MeV, respectively. In comparison, the half-life of the isotope ^{267}108 has been measured [12] to be 19^{+20}_{-10} ms with an α-decay energy of 9.74-9.87 MeV. The half-life for the Z=108 isotope is 3 orders of magnitude smaller than those of the Z=106 isotopes. This difference of about 3 orders of magnitude between Z=106 and Z=108 is also shown in the results of the RMF theory in Fig. 8, where an enhancement at N=166 is seen. The α-decay energies in RMF theory (Fig. 9) are consistent with the experimental values. Thus, the above experimental data would be consistent with a strong shell gap at Z=106 in the single-particle spectrum in the RMF theory.

Another shell gap at proton number Z=114 is also predicted in the RMF theory. A similar prediction for closed proton shell is made by other theories [2, 3]. However, owing to an enhanced stability and thus a higher life-time for decay, proton number Z=106 may be preferred in the synthesis of nuclei. The shell gaps in neutrons as well as in protons would augment the stability of nuclei. From this point of view, the nucleus with Z=106

and N=166 seems to provide a good indication for a 'double-magic' nucleus amidst the nuclei where a significant deformation is prevalent. In other words, the region Z=106 and N=166 may provide an island of extra stability. It is noteworthy that deformation acquired by nuclei near the above magic region is minimal as compared to their heavier or lighter counterparts.

In conjunction with the proton number Z=114, an unambiguous shell closure appears at N=184 in the RMF theory, whereby most of the nuclei become spherical. This shell closure has also been predicted by the the macroscopic-microscopic calculations of Möller and Nix [3]. In the RMF theory, the combination Z=114 and N=184 constitutes another 'double-magic' number. Thus, RMF theory reinforces the prediction for another region of extra stability in the domain of superheavy nuclei.

It may be instructive to make a comparison of the RMF predictions with other theories and models. Some of the predictions about shell closures as well as on the existence of an island of extra-stable deformed nuclei in the RMF theory are consistent with the predictions of the macroscopic-microscopic approaches. It is noteworthy that the RMF theory, the FRDM and the Nilsson-Strutinsky approach [2], all indicate strong shell closures at Z=114 and N=184. In other regions, however, various predictions seem to differ. Most notable amongst these is in the middle of the major shell N=184, i.e. in the region of the deformed shell whereby a shell closure appears at N=166 in RMF theory with a prolate deformation $\beta_2 = 0.18$. In comparison, the FRDM predicts a deformed shell closure at N=162 and at N=164 with a corresponding β_2 about 0.22. The prediction of shell closure in FRDM at N=162 is in accord with the prediction of the Nilsson-Strutinsky approach [2] where a deformed shell closure has also been surmised at N=162. The closeness in this prediction of the macroscopic-microscopic approaches FRDM and Nilsson-Strutinsky might stem from the similarity in the calculation of the shell effects.

The FRDM also predicts large gaps in the single-particle energies at Z=104, 106, 108 and 110 corresponding to a prolate deformation. In contrast, the RMF theory predicts a strong shell closure at Z=106. In the Nilsson-Strutinsky approach, on the other hand, the deformed shell closure occurs at Z=108.

In conclusion, some of the predictions of the microscopic RMF theory are consistent with those of the FRDM and Nilsson-Strutinsky approach whereas some other predictions of our approach differ from the latter. It is worth pointing out that the latter models employ a large number of parameters which are fitted to a large body of data. In comparison, the RMF theory is based upon a smaller number of parameters fitted to a limited data. The fact that the RMF theory using only a few parameters has been able to describe nuclear properties all over the periodic table provides a confidence in its predictions.

6 Acknowledgment

The authors are thankful to Fedja Ivanyuk for his help in the calculation of the shell corrections. One of the authors (G.A.L) acknowledges support by the European Union under the contracts HCM-EG/ERB CHBICT-930651 and TMR-EU/ERB FMBCICT-950216. Partial support from the Bundesministerium für Forschung und Technologie under the project 06TM734 (6) is acknowledged.

References

[1] J.R. Nix, Physics Today 1972 p. 30.

[2] A. Sobiczewski, Sov. J. Part. Nucl. **25** (1994) 119.

[3] P. Möller, J.R. Nix, J. Phys. **G20** (1994) 1681.

[4] P. Ambruster, Ann. Rev. Nucl. Part. Sci. **35** (1985) 135.

[5] Yu. Ts. Oganessian, and Yu. A. Lazarev, in *Treaties on Heavy-Ion Science*, Vol. 4, edited by D.A. Bromley (Plenum Press, N.Y., 1985) p. 3.

[6] G. Münzenberg, Rep. Prog. Phys. **51** (1988) 57.

[7] P. Ambruster, in Proc. of Inter. Conf. on Nuclear Shapes and Nuclear Structure at Low Excitation Energies, Antibes (France), (eds.) M. Vergnes, D. Goutte, P.H. Heenen and J. Sauvage, Editions Frontieres, (1994) p. 365.

[8] Yu. Ts. Oganessian, Nucl. Phys. **A583** (1995) 823.

[9] S. Hofmann et al., Z. Phys. **A350** (1995) 277.

[10] S. Hofmann et al., Z. Phys. **A354** (1996) 229.

[11] Yu. A. Lazarev et al., Phys. Rev. Lett. **73** (1994) 624.

[12] Yu. A. Lazarev et al., Phys. Rev. Lett. **75** (1995) 1903.

[13] Yu. A. Lazarev et al,. Dubna Report No. E7-95-552 (submitted to Phys. Rev. C).

[14] Z. Patyk and A. Sobiczewski, Nucl. Phys. **A533** (1991) 132.

[15] Z. Patyk and A. Sobiczewski, Phys. Lett. **256B** (1991) 307.

[16] M. Beiner, H. Flocard and M. Veneroni, Phys. Scr. **10A** (1974) 84.

[17] P. Quentin and H. Flocard, Ann. Rev. Nucl. Part. Sci. **28** (1978) 523.

[18] Y.K. Gambhir, P. Ring, and A. Thimet, Ann. Phys. (N.Y.) **198** (1990) 132.

[19] J. Dobaczewski, private communication to P. Ring

[20] P.G. Reinhard, Rep. Prog. Phys. **55** (1989) 439.

[21] M.M. Sharma, M.A. Nagarajan, and P. Ring, Phys. Lett. **B312** (1993) 377

[22] G.A. Lalazissis and M.M. Sharma, Nucl. Phys. **A586** (1995) 201.

[23] G.A. Lalazissis, M.M. Sharma and P. Ring, Nucl. Phys. **A597** (1996) 35.

[24] M.M. Sharma, G.A. Lalazissis, W. Hillebrandt, and P. Ring, Phys. Rev. Lett. **72** (1994) 1431.

[25] M.M. Sharma, G.A. Lalazissis, and P. Ring, Phys. Lett. **B317** (1993) 9.

[26] H. Kucharek and P. Ring Z. Phys. **A339** (1991) 23.

[27] B.D. Serot and J.D. Walecka, Adv. Nucl. Phys. **16** (1986) 1.

[28] B.D. Serot, Rep. Prog. Phys. **55** (1992) 1855.

[29] J. Boguta and A.R. Bodmer, Nucl. Phys. **A292** (1977) 413.

[30] J. Decharge and D. Gogny, Pfys. Rev. **C 21** (1980) 1568.

[31] J.D. Talman, Nucl. Phys. **A141** (1970) 273.

[32] P. Möller, J.R. Nix, Nucl. Phys. **A536** (1992) 20.

[33] G. Audi and A.H. Wapstra, Nucl. Phys. **A565** (1993) 1.

[34] P. Möller, J.R. Nix, W.D. Myers, and W.J. Swiatecki, Atomic Data and Nuclear Data Tables 59 (1995) 185.

[35] Y. Aboussir, J.M. Pearson, A.K. Dutta, and F. Tondeur, Atomic Data and Nuclear Data Tables 61 (1995) 127.

[36] V.E. Viola Jr. and G.T. Seaborg, J. Inorg. Nucl. Chem. **28** (1966) 741.

[37] A. Sobiczewski, Z. Patyk and S. Cwiok, Phys. Lett. **224B** (1989) 1.

[38] J. Libert and P. Quentin, Phys. Rev. **C25** (1982) 571.

[39] M. Brack, J. Damgaard, A.S. Jensen, H.C. Pauli, V.M. Strutinsky, C.Y.Wong; Rev. Mod. Phys. **44** (1972) 320.

Figure Captions

Fig. 1 The two-neutron separation energies S_{2n} obtained from the RHB calculations with spherical configuration for nuclei with atomic numbers Z=100 to Z=114 for neutron numbers (a) N=158-176 and (b) N=178-190.

Fig. 2 The two-proton separation energies S_{2p} obtained from the RHB calculations with spherical configuration for nuclei with atomic numbers Z=100 to Z=114 for neutron numbers (a) N=158-178 and (b) N=180-188.

Fig. 3 The S_{2n} values from FRDM for nuclei with neutron numbers (a) N=158-170 and (b) N=180-188. The S_{2p} values from FRDM for nuclei with neutron numbers (c) N=156-170 and (d) N=180-184, as taken from ref. [34].

Fig. 4 The same as in Fig. 3, but from the ETF-SI as taken from ref. [35].

Fig. 5 The neutron pairing energy obtained from the RHB calculations for spherical configurations.

Fig. 6 The proton pairing energy obtained from the RHB calculations for spherical configurations.

Fig. 7 The alpha-decay half life T_a obtained from Viola-Seaborg systematics using the results of the RHB calculations.

Fig. 8 (a) S_{2n} and (b) T_a obtained from the deformed RMF calculations with 20 oscillator shells.

Fig. 9 The Q_α values for deformed nuclei about N=164 with Z=106 and Z=108.

Fig. 10 The neutron and proton single-particle energies for nuclei with Z=106 and Z=108 with neutron number N=162 obtained from deformed RMF calculations.

Fig. 11 The same as in Fig 10, but for N=164.

Fig. 12 The same as in Fig 10, but for N=166.

Fig. 13 The neutron and proton single-particle energies for nuclei with Z=106, 108, 110 and 114 with neutron number N=184.

Table 1: The relevant parameters of the Gogny interaction D1 used in the present work. The range is in fermis and the constants W,B,H,M are in MeV.

i	range	W_i	B_i	H_i	M_i
1	0.7	-402.4	-100.0	-496.2	-23.56
2	1.2	-21.3	-11.77	37.27	-68.81

Table 2: The parameters of the force NL-SH. All the masses are in MeV, while g_2 is in fm^{-1}. The other coupling constants are dimensionless.

$\mathrm{M} = 939.0$	$m_\sigma = 526.059$	$m_\omega = 783.0$	$m_\rho = 763.0$	
$g_\sigma = 10.444$	$g_\omega = 12.945$	$g_\rho = 4.383$	$g_2 = -6.9099$	$g_3 = -15.8337$

Table 3: The β_2 and β_4 deformation parameters calculated in the RMF theory with the NL-SH force. Values from the mass models FRDM and ETF-SI are also shown for comparison

		β_2			β_4		
Z	N	RMF	FRDM	ETF-SI	RMF	FRDM	ETF-SI
102	156	0.246	0.228	0.270	-0.015	-0.019	0.000
	158	0.247	0.228	0.250	-0.029	-0.028	-0.020
104	158	0.251	0.229	0.250	-0.041	-0.037	-0.020
	160	0.253	0.220	0.260	-0.054	-0.046	-0.050
	162	0.247	0.230	0.260	-0.060	-0.069	-0.050
	164	0.197	0.221	0.250	-0.033	-0.072	-0.040
	166	0.179	0.201	0.250	-0.034	-0.067	-0.040
106	158	0.251	0.229	0.260	-0.047	-0.044	-0.050
	160	0.254	0.230	0.260	-0.060	-0.061	-0.050
	162	0.248	0.231	0.260	-0.065	-0.078	-0.050
	164	0.197	0.221	0.260	-0.039	-0.080	-0.050
	166	0.183	0.201	0.250	-0.042	-0.074	-0.060
	168	0.168	0.164	0.230	-0.043	-0.054	-0.050
108	160	0.236	0.230	0.260	-0.052	-0.069	-0.050
	162	0.211	0.231	0.260	-0.042	-0.086	-0.080
	164	0.198	0.222	0.250	-0.045	-0.089	-0.070
	166	0.185	0.212	0.250	-0.049	-0.091	-0.070
	168	0.173	0.164	0.410	-0.053	-0.063	0.070
110	166	0.182	0.212	0.410	-0.058	-0.091	0.070
112	166	0.180	0.164	0.430	-0.065	-0.063	0.070
	168	0.173	0.080	0.430	-0.071	-0.006	0.070

Table 4: The binding energies (in MeV) for some superheavy nuclei with N=184 obtained in the deformed RMF calculations with the interaction NL-SH. Predictions from the mass models FRDM and ETF-SI are also shown for comparison. The quadrupole deformation β_2 obtained in the RMF calculations along-with the predictions from FRDM and ETF-SI. The RMF theory predicts a spherical shape for these nuclei.

	B.E			β_2		
A	NL-SH	FRDM	ETF-SI	NL-SH	FRDM	ETF-SI
$^{290}106$	-2078.65	-2074.10	-2078.25	-0.003	0.000	0.000
$^{292}108$	-2092.15	-2088.56	-2091.60	-0.004	0.000	0.000
$^{294}110$	-2104.38	-2101.67	-2103.60	-0.005	0.000	-0.010
$^{298}114$	-2125.00	-2123.30	-2122.86	-0.005	0.000	-0.010

Table 5: The shell corrections calculated in the RMF theory for a number of heavy nuclei. The effect due to pairing has been included in obtaining the shell energies.

Z/N	154	156	158	160	162	164	166	168
104	-6.22	-6.32	-6.47	-6.79	-6.16	-3.76	-3.35	-2.60
106	-6.44	-6.97	-7.53	-8.05	-7.27	-4.88	-4.58	-3.64
108	-6.54	-7.12	-7.32	-7.12	-6.28	-5.74	-5.43	-4.40
110	-6.47	-6.20	-6.39	-6.21	-5.86	-5.85	-6.12	-5.32
112	-4.43	-5.40	-5.67	-5.60	-5.73	-6.37	-7.09	-6.49
114	-3.86	-4.71	-4.87	-4.79	-4.97	-5.91	-6.79	-6.66
116	-3.41	-4.21	-4.23	-4.00	-3.96	-4.84	-5.78	-5.75

Figure 1

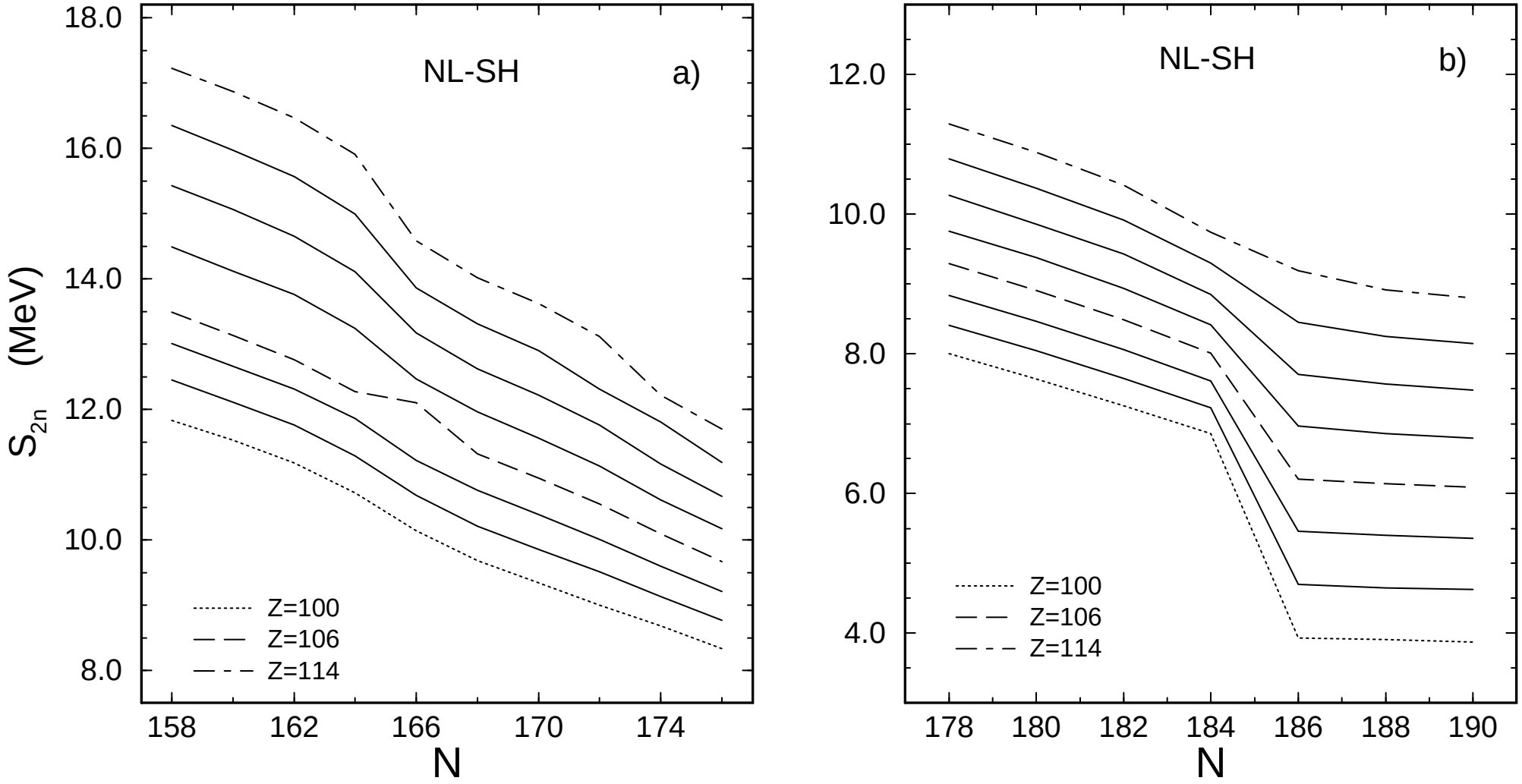
NL-SH
a)
S_{2n} (MeV)
18.0
16.0
14.0
12.0
10.0
8.0
158
162
166
170
174
N
Z=100
Z=106
Z=114
NL-SH
b)
12.0
10.0
8.0
6.0
4.0
178
180
182
184
186
188
190
N
Z=100
Z=106
Z=114

Figure 2

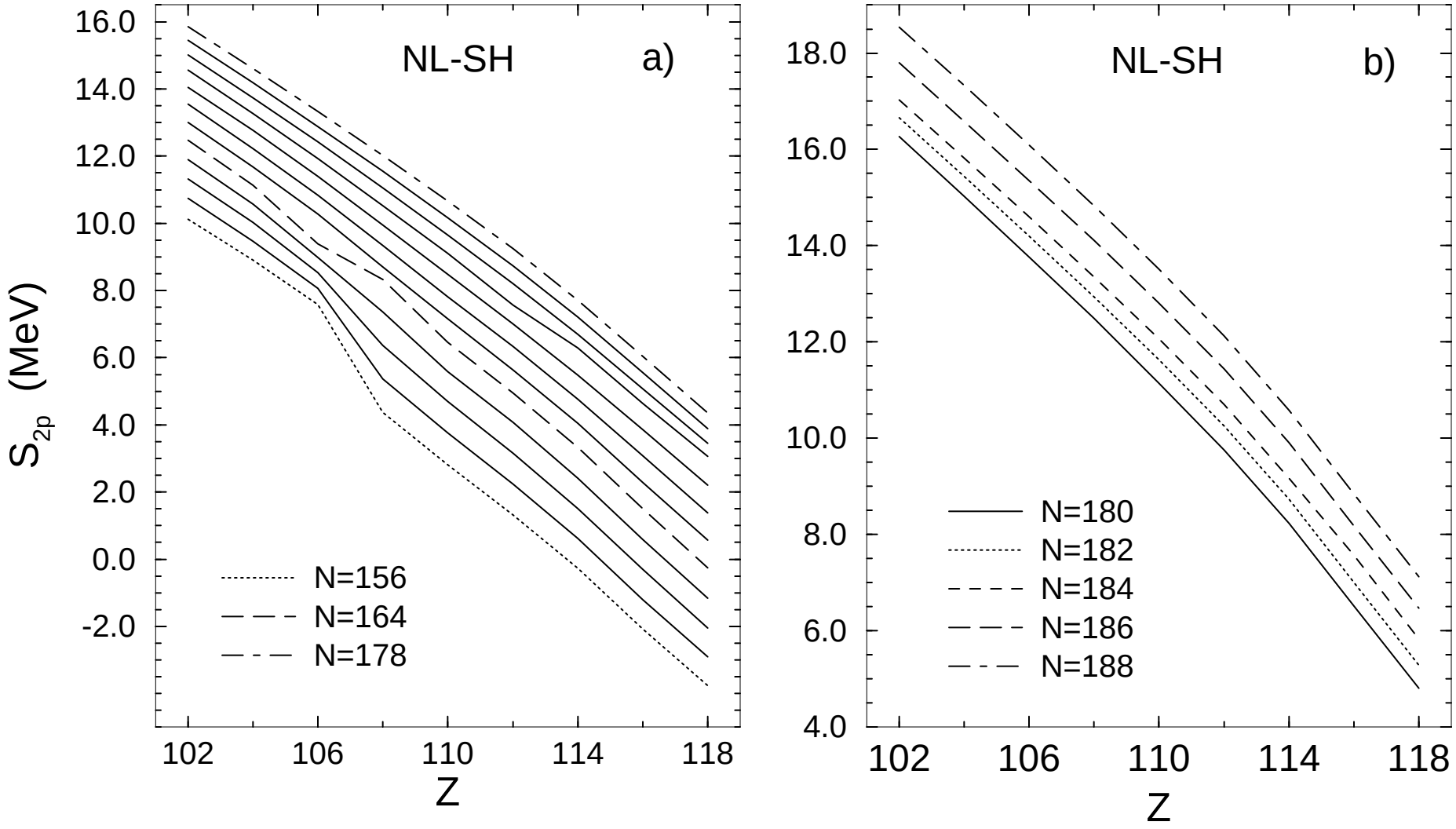
NL-SH
a)
S_{2p} (MeV)
16.0
14.0
12.0
10.0
8.0
6.0
4.0
2.0
0.0
-2.0
N=156
N=164
N=178
102
106
110
114
118
Z
NL-SH
b)
18.0
16.0
14.0
12.0
10.0
8.0
6.0
4.0
N=180
N=182
N=184
N=186
N=188
102
106
110
114
118
Z

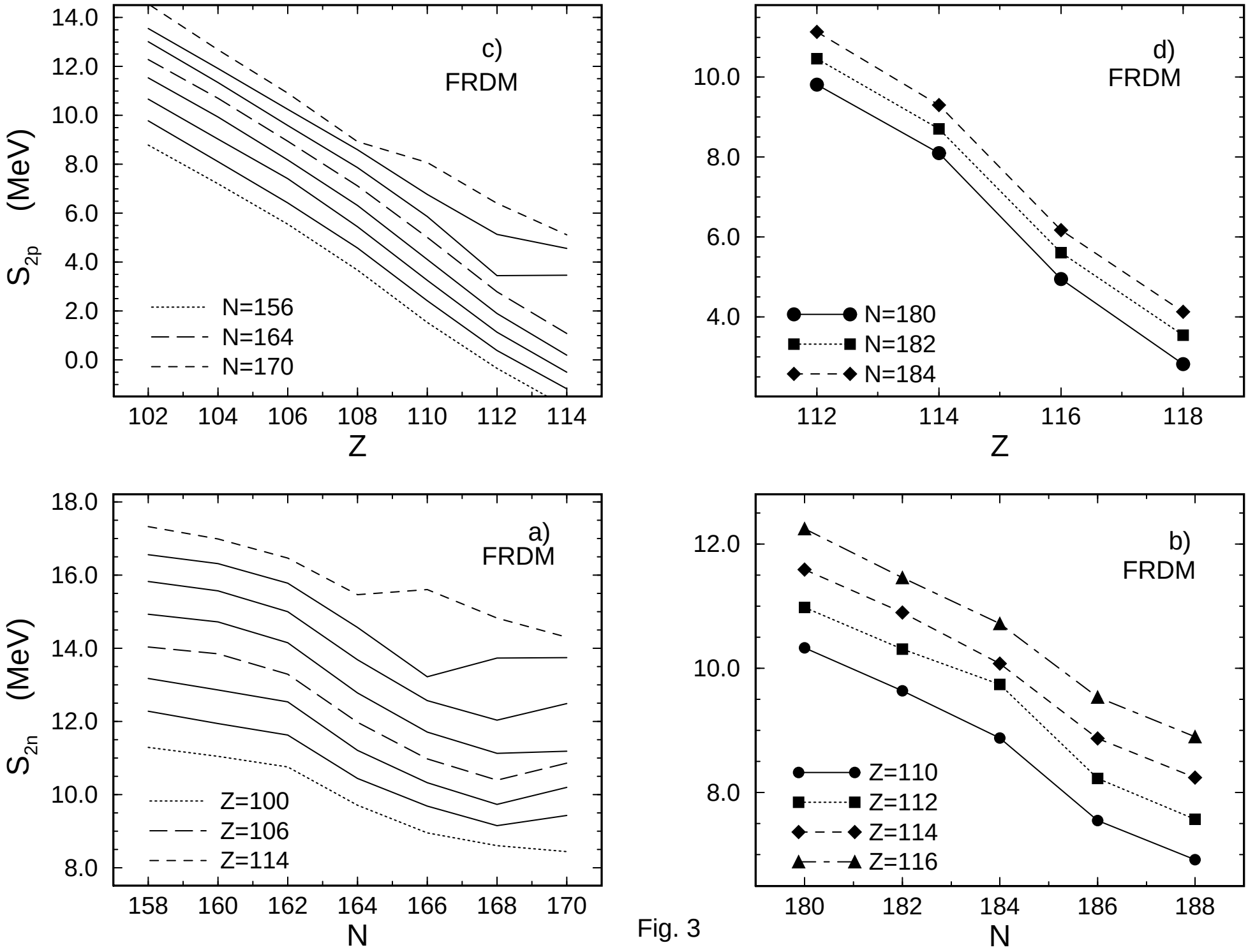
c)
FRDM
S_{2p} (MeV)
Z
N=156
N=164
N=170
d)
FRDM
N=180
N=182
N=184
Z
a)
FRDM
S_{2n} (MeV)
N
Z=100
Z=106
Z=114
b)
FRDM
Z=110
Z=112
Z=114
Z=116
N

Fig. 3

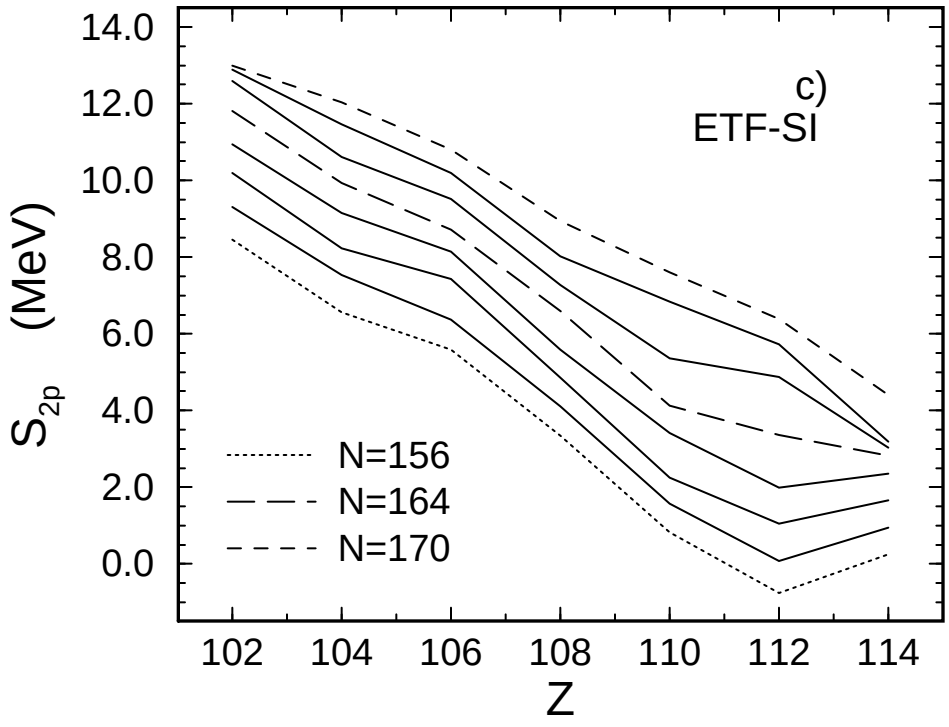
c)
ETF-SI
N=156
N=164
N=170
S_{2p} (MeV)
Z

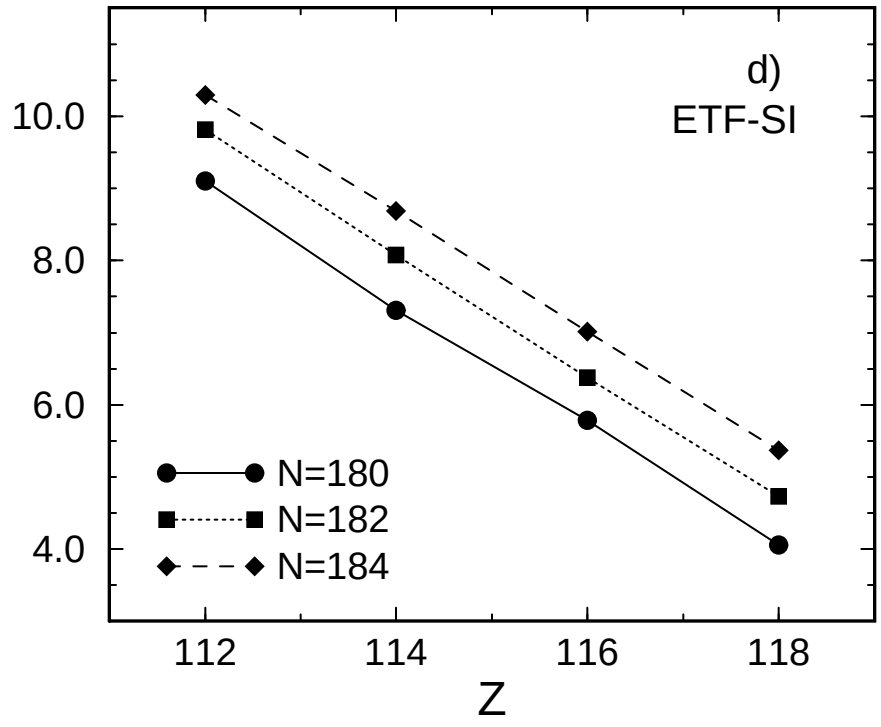
d)
ETF-SI
N=180
N=182
N=184
Z

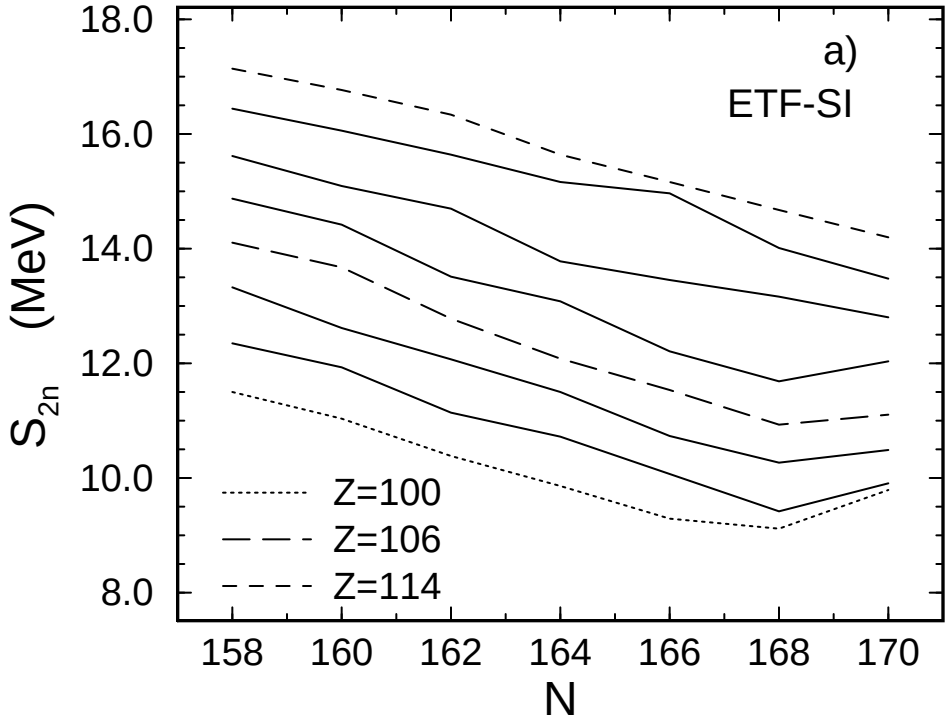
a)
ETF-SI
Z=100
Z=106
Z=114
S_{2n} (MeV)
N

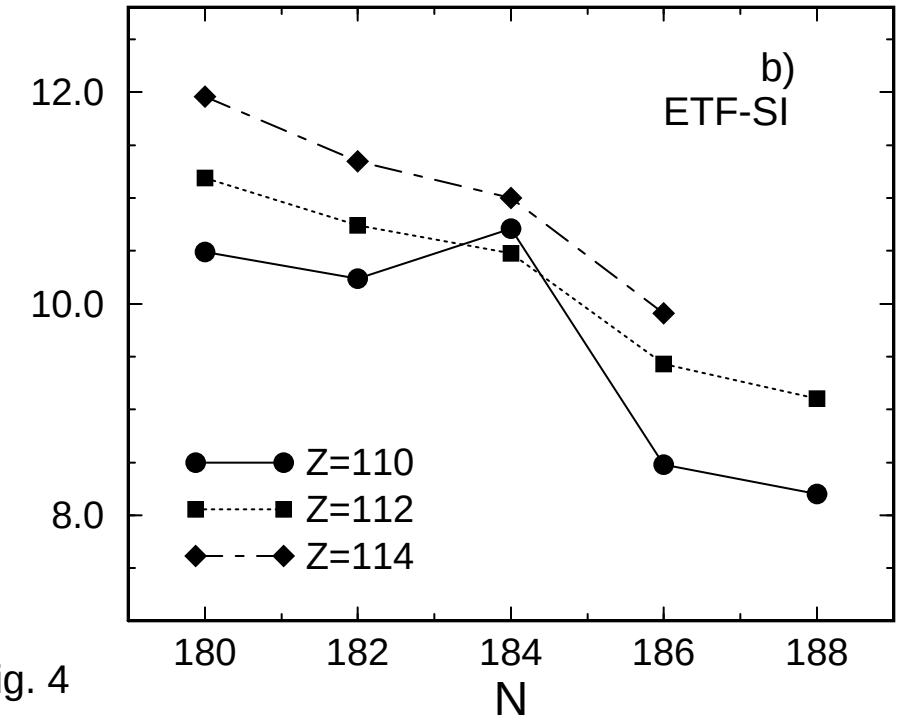
b)
ETF-SI
Z=110
Z=112
Z=114
N

Fig. 4

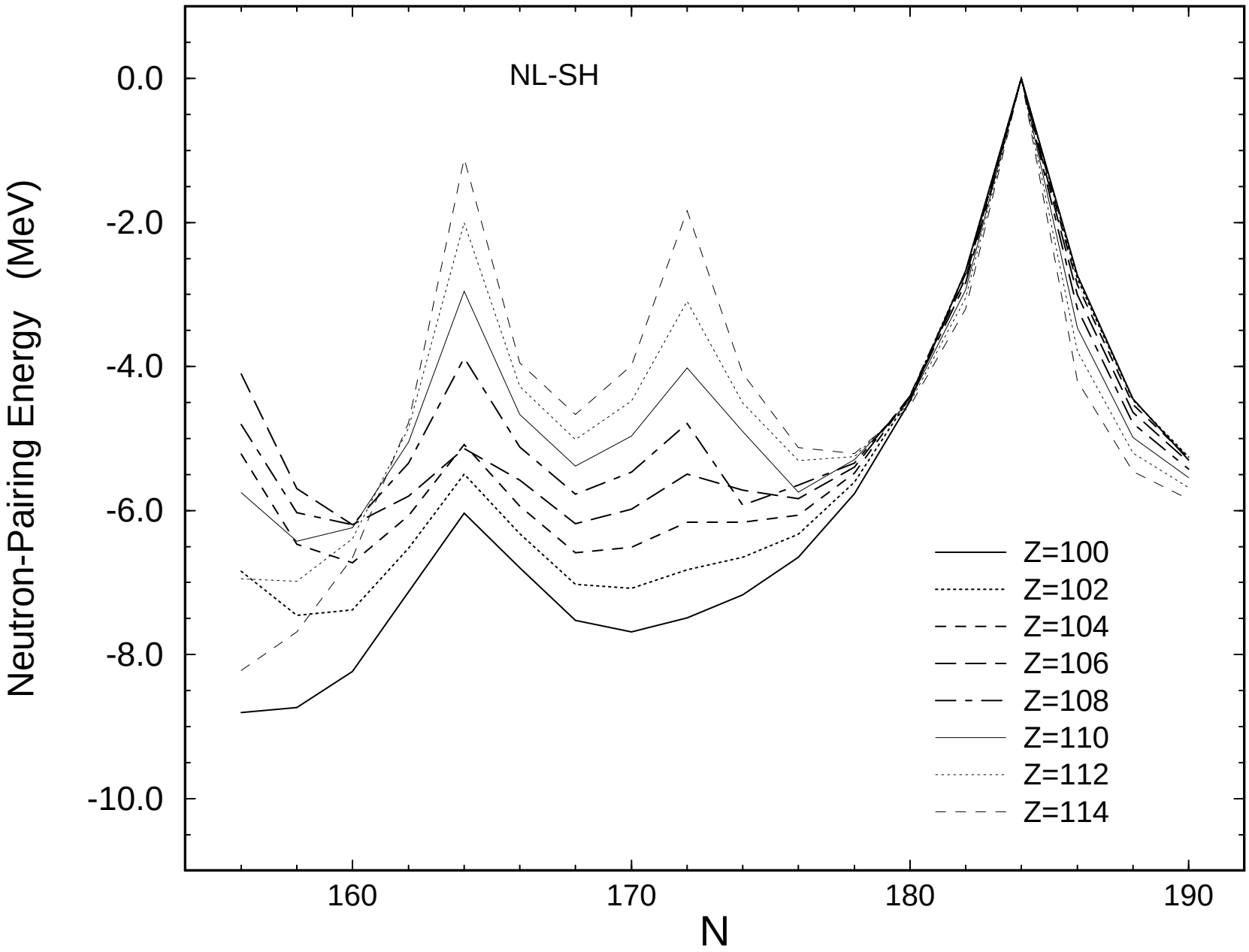
NL-SH
Neutron-Pairing Energy (MeV)
0.0
-2.0
-4.0
-6.0
-8.0
-10.0
160
170
180
190
N
Z=100
Z=102
Z=104
Z=106
Z=108
Z=110
Z=112
Z=114

Figure 5

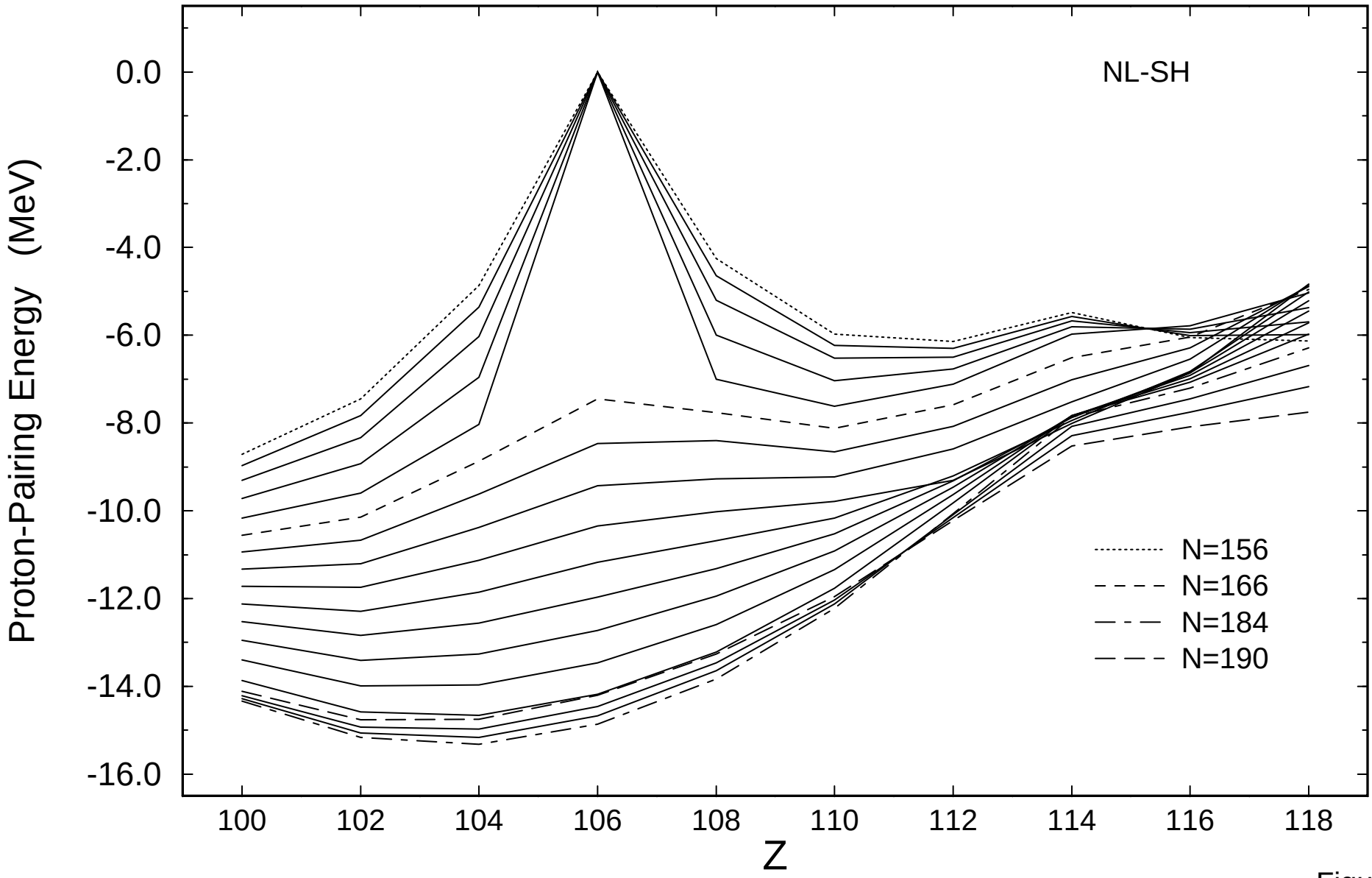
NL-SH
Proton-Pairing Energy (MeV)
0.0
-2.0
-4.0
-6.0
-8.0
-10.0
-12.0
-14.0
-16.0
100
102
104
106
108
110
112
114
116
118
Z
N=156
N=166
N=184
N=190

Figure 6

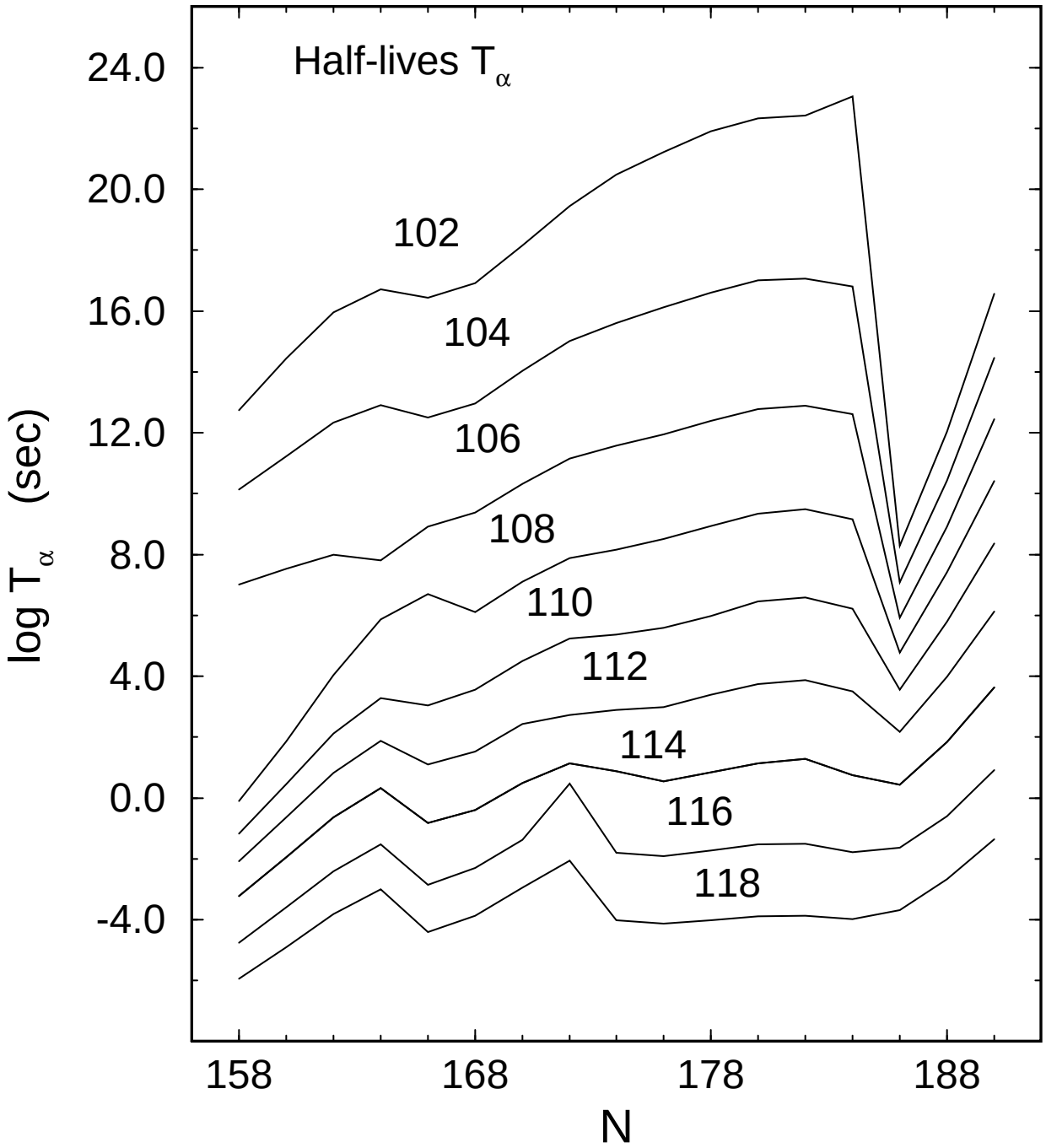
Half-lives T_α
24.0
20.0
16.0
12.0
8.0
4.0
0.0
-4.0
log T_α (sec)
102
104
106
108
110
112
114
116
118
158
168
178
188
N

Figure 7

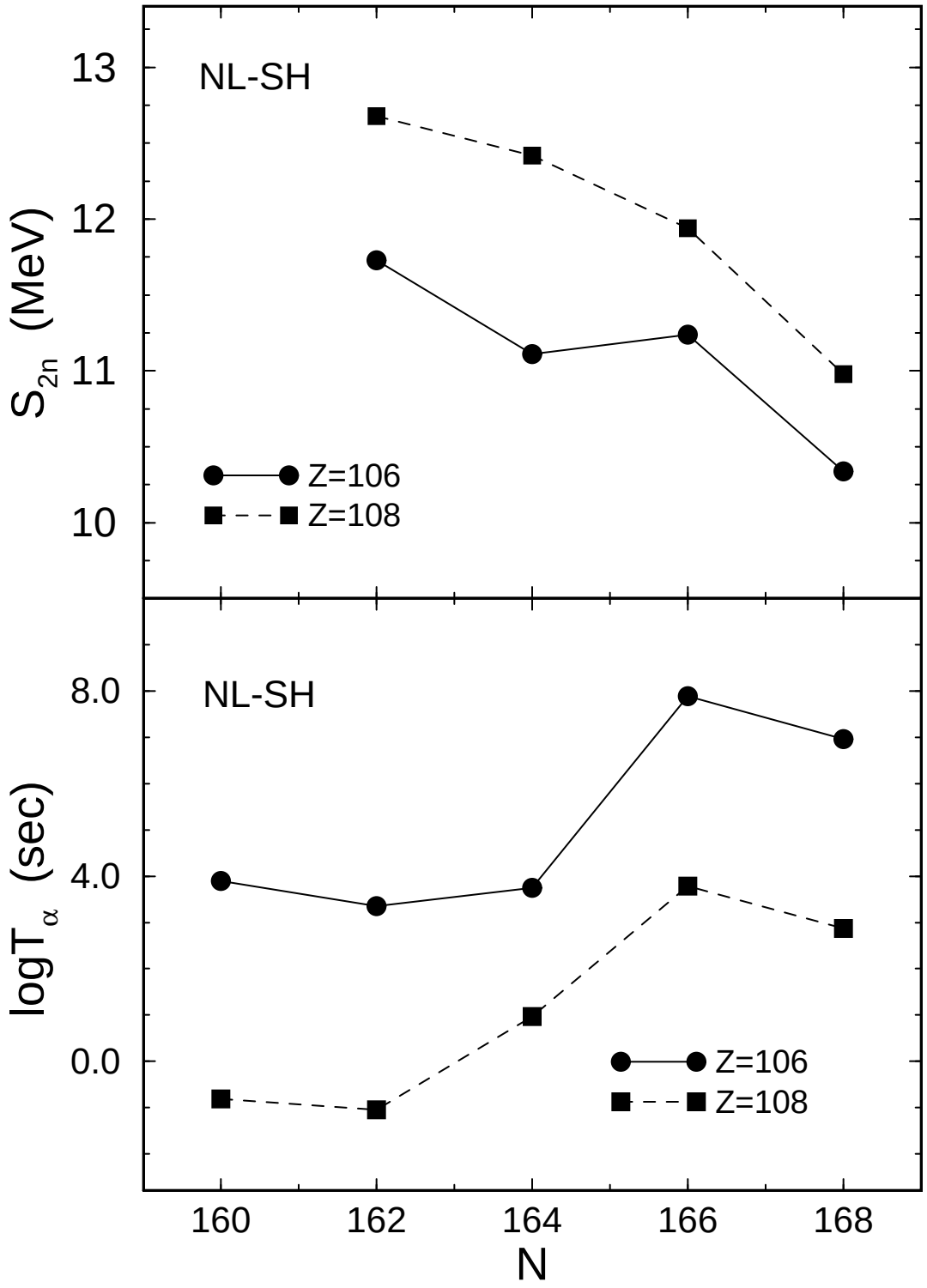
NL-SH
13
12
11
10
S_{2n} (MeV)
Z=106
Z=108
NL-SH
8.0
4.0
0.0
$\log T_\alpha$ (sec)
Z=106
Z=108
160
162
164
166
168
N

Figure 8

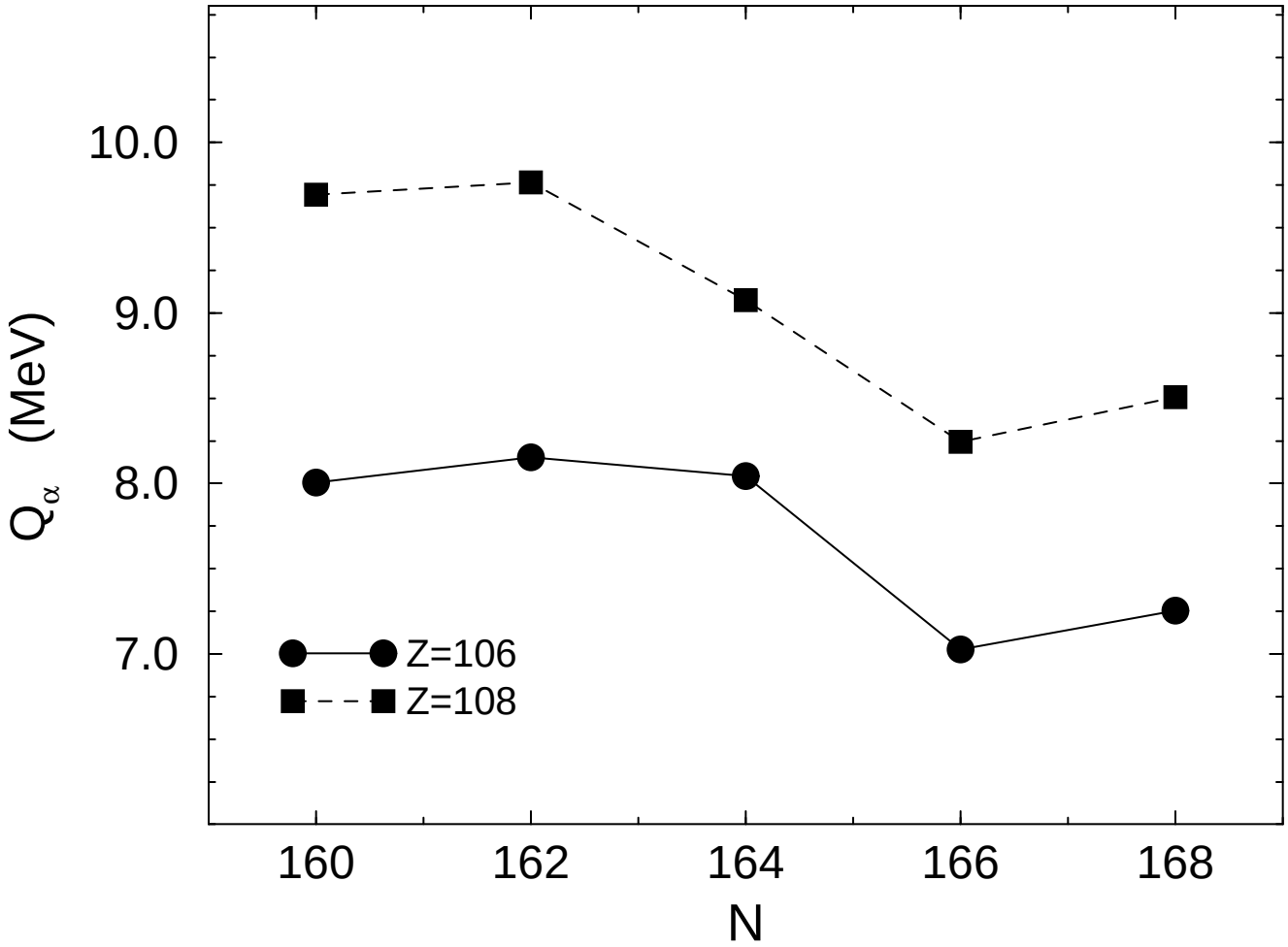

Figure 9

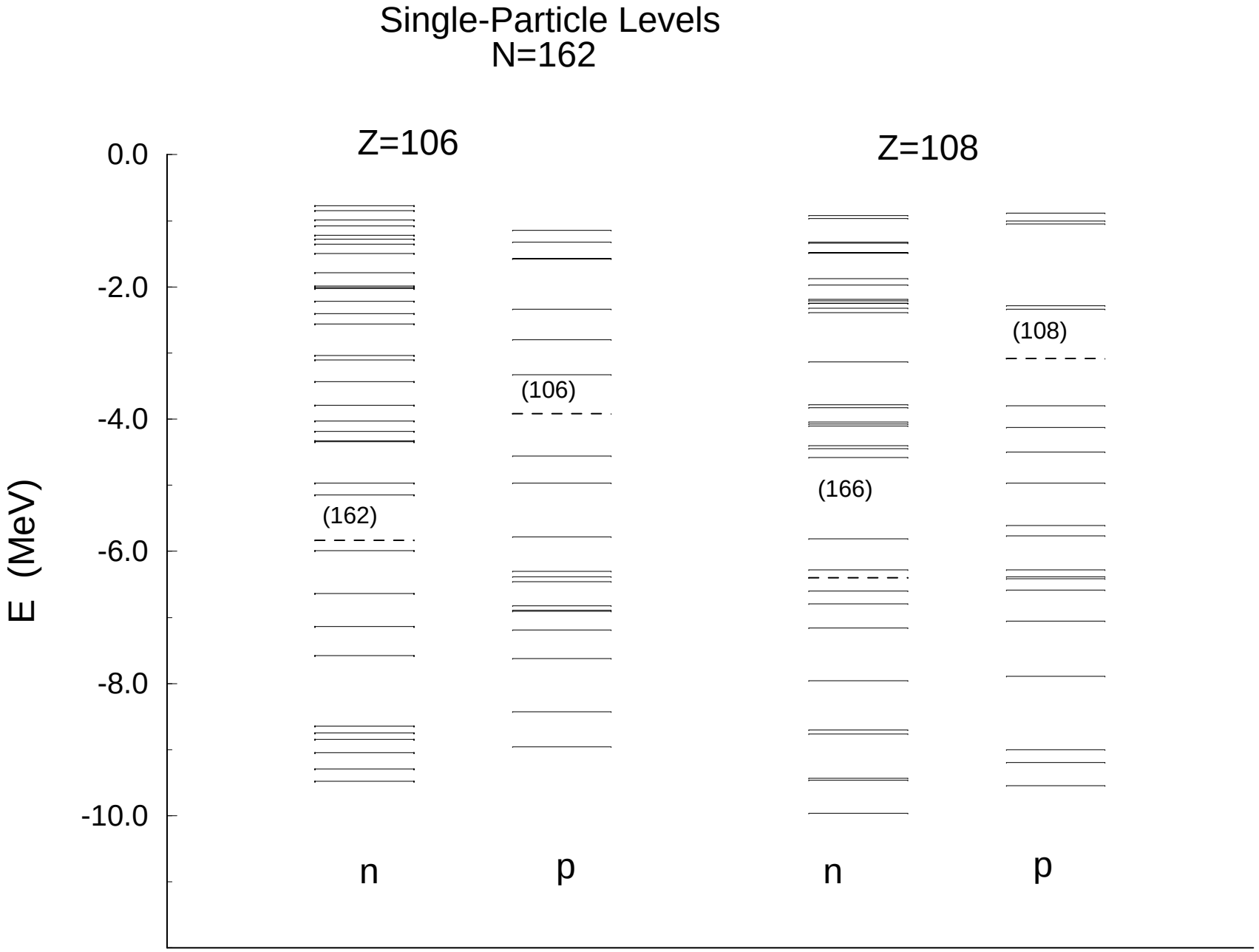
Single-Particle Levels
N=162
Z=106
Z=108
0.0
-2.0
-4.0
-6.0
-8.0
-10.0
E (MeV)
(162)
(106)
(166)
(108)
n
p
n
p

Figure 10


Single-Particle Levels
N=164
Z=106
Z=108
0.0
-2.0
-4.0
-6.0
-8.0
-10.0
E (MeV)
(166)
(106)
(166)
(108)
n
p
n
p

Figure 11

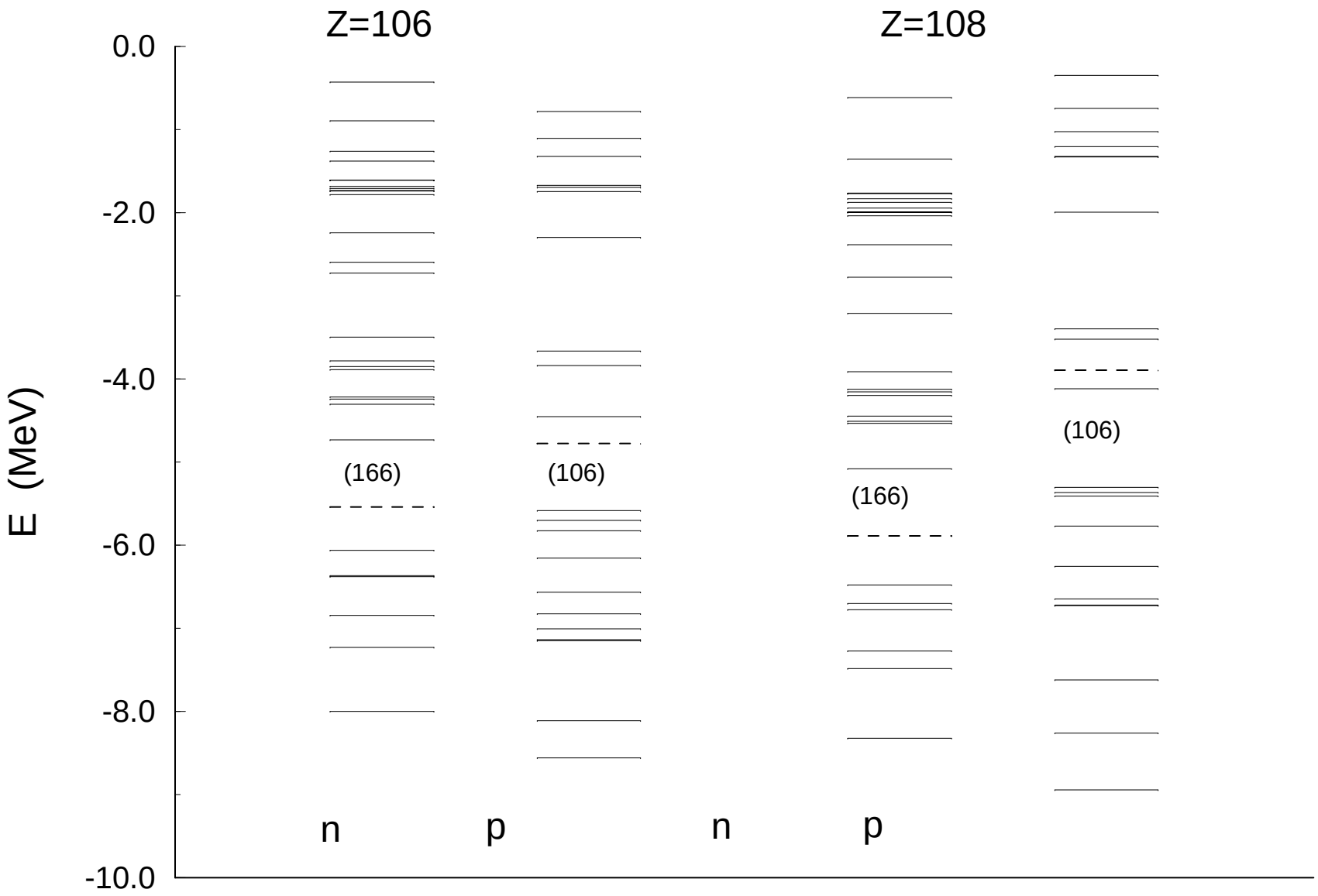
Single-Particle Levels
N=166
Z=106
Z=108
0.0
-2.0
-4.0
-6.0
-8.0
-10.0
E (MeV)
(166)
(106)
(166)
(106)
n
p
n
p

Figure 12

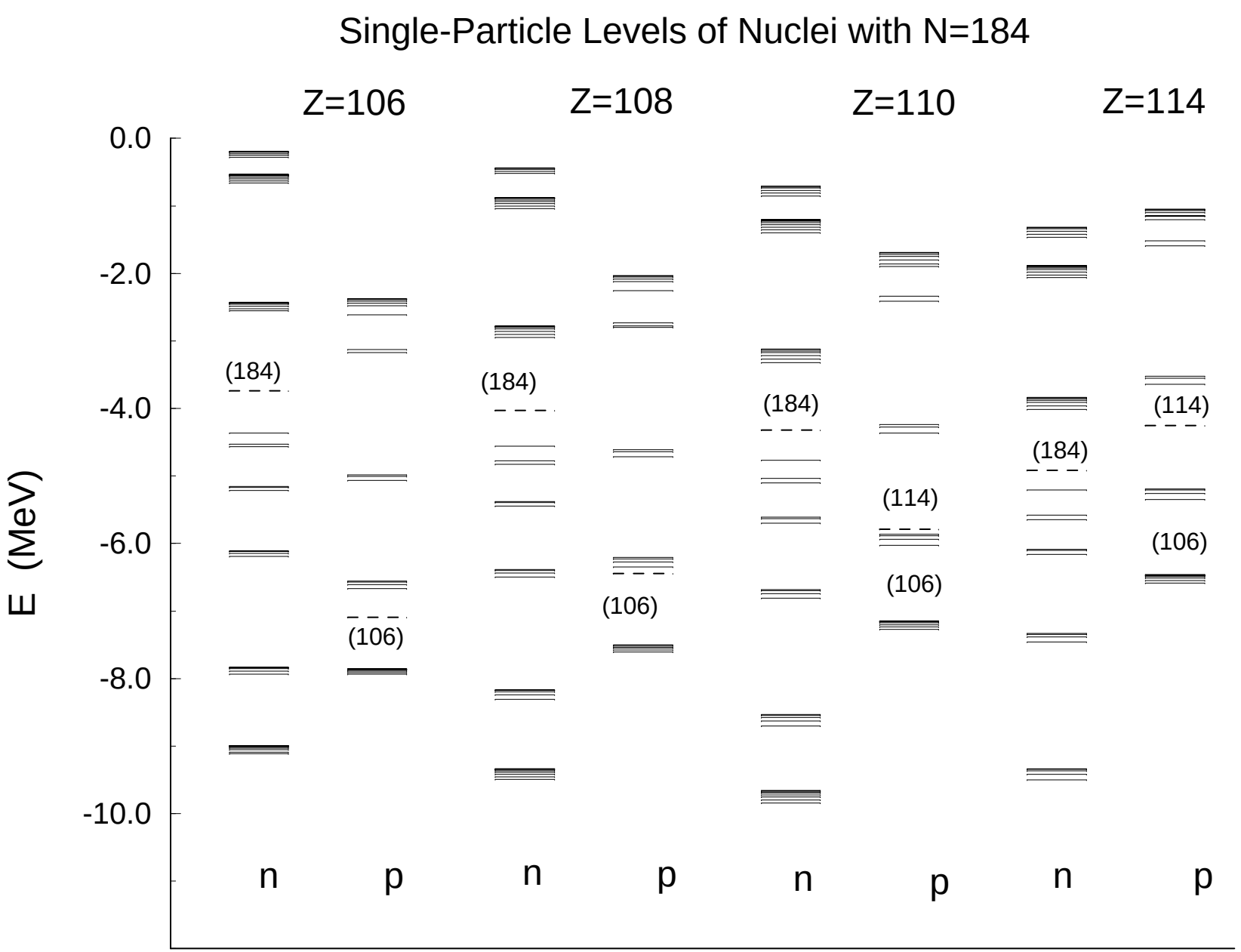
Single-Particle Levels of Nuclei with N=184
Z=106
Z=108
Z=110
Z=114
0.0
-2.0
-4.0
-6.0
-8.0
-10.0
E (MeV)
(184)
(106)
(184)
(106)
(184)
(114)
(106)
(184)
(114)
(106)
n
p
n
p
n
p
n
p

Figure 13